Structures 71 (2025) 108109

Contents lists available at ScienceDirect

Structures

journal homepage: www.elsevier.com/locate/structures

Beam-column connections in GFRP-RC moment resisting frames: A review of seismic behaviour and key parameters

Mohamed H. El-Naqeeb [a,b,1], Reza Hassanli [a,*,2], Yan Zhuge [a,3], Xing Ma [a,4], Milad Bazli [c,5], Allan Manalo [d,6]

[a] University of South Australia, UniSA STEM, Mawson Lakes, SA 5095, Australia
[b] Badr University in Cairo, School of Engineering and Technology, Cairo 11829, Egypt
[c] Faculty of Science and Technology, Charles Darwin University, Darwin, Australia
[d] Center for Future Materials, School of Engineering, University of Southern Queensland, QLD 4350, Australia

ARTICLE INFO

Keywords:
Beam-column connection
GFRP
Joint shear strength
Moment resisting frames
Seismic design

ABSTRACT

Glass Fibre Reinforced Polymer (GFRP) bars have emerged as an effective alternative to steel as internal reinforcements in concrete structures. Its application in individual reinforced concrete (RC) members has been widely implemented. However, the use of GFRP bars for structures built in regions with high seismic activities is very limited because of the linear elastic behaviour of this reinforcing material. The major reason contributing to this is the lack of seismic provisions for connections in GFRP-reinforced moment-resisting frames (GFRP-RC MRFs) in available design standards because of the limited understanding of its seismic performance. This comprehensive review will provide a thorough understanding of the performance of GFRP-RC MRFs in seismic regions, the challenges and the potential advantages and disadvantages. The design parameters governing the connection response were identified and evaluated to help in the appropriate design of the connections of MRFs. This state-of-the-art review found that the GFRP-RC beam-column sub-assemblages can reach a 4 % drift without strength reduction, resulting in a pseudo-ductile behaviour that provides warnings of impending failure. However, at the drift allowance of 2.5 % for conventional RC structures, it was recognized that the design capacity may not always be reached. Additionally, the GFRP-RC beam-column subassembly can demonstrate minimal damage after earthquakes and can withstand repeated earthquake loads without requiring repair, thereby minimizing repair costs. However, this resilience comes at the expense of ductility and energy dissipation capacity reduction. Therefore, it is advisable to prevent joint failure and employ well-over reinforced structural elements to facilitate a more gradual failure by keeping the reinforcement's stress of the beams well below its capacity. Besides, incorporating replaceable external damping systems can enhance the energy dissipation capacity, especially considering the nearly elastic behaviour of GFRP-RC and their low level of damage. The study also outlined design guidelines for beam-column connections, including joint shear strength, anchorage details, and the column-to-beam flexural capacity ratio. This synthesis of existing literature points to the potential use of GFRP-RC MRFs in seismic regions and highlights their shortcomings, current issues, the gaps regarding the better understanding of GFRP-RC MRFs performance as well as guiding future research toward establishing seismic provisions for GFRP-RC MRFs.

* Corresponding author.
E-mail addresses: mohamed.el-naqeeb@mymail.unisa.edu.au, mohamed.hafez@buc.edu.eg (M.H. El-Naqeeb), reza.hassanli@unisa.edu.au (R. Hassanli), yan.zhuge@unisa.edu.au (Y. Zhuge), xing.ma@unisa.edu.au (X. Ma), milad.bazli@cdu.edu.au (M. Bazli), allan.manalo@usq.edu.au (A. Manalo).
[1] ORCID: https://orcid.org/0000-0002-0573-2978
[2] ORCID: https://orcid.org/0000-0001-5855-6405
[3] ORCID: https://orcid.org/0000-0003-1620-6743
[4] ORCID: https://orcid.org/0000-0001-5488-5252
[5] ORCID: https://orcid.org/0000-0001-9027-6155
[6] ORCID: https://orcid.org/0000-0003-0493-433X

https://doi.org/10.1016/j.istruc.2024.108109
Received 30 August 2024; Received in revised form 23 November 2024; Accepted 19 December 2024
Available online 30 December 2024

1. Introduction

Beam-column joint is the most critical component in a moment-resisting frame (MRF) that needs to be well-designed and detailed to ensure the integrity and safety of the lateral and gravitational load-transferring system [1,2]. Joints can be classified according to their location as interior, exterior, and knee connection (see Fig. 1a). While the beam and column elements can be simply designed to meet the design requirements, the design of the joint region is more challenging due to the complicated stress-transferring mechanism in the joint. Also, due to the discontinuity of strains, the joint region is usually subjected to stress concentration with much higher stress than connected members [2]. Inadequate joint strength can cause partial and total collapse of the MRF [3,4]. To avoid such failure, seismic provisions have been considered in international design standards for steel reinforced concrete (RC) [5–7] including four criteria namely; strong column weak beam concept, adequate confining reinforcement, proper anchorage, and sufficient joint shear strength.

Proper design of the joint can be achieved by ensuring sufficient joint shear strength, providing adequate joint shear reinforcement and proper anchorage of beam bars. Subsequently, the connected members are expected to reach their ultimate capacity prior to the failure of the joint. This can occur through one of two potential failure mechanisms. The first is the weak column strong beam mechanism which involves the development of a plastic hinge in the column before the beams. This causes undesirable excessive sway and progressive collapse. Conversely, with a strong column weak beam mechanism, plastic hinges are expected to be formed in the beams before the column [8]. This ductile failure mechanism involves a uniform distribution of drift over the structure height, as shown in Fig. 1b. The latter is commonly adopted in the design of MRFs under lateral loads [5–7] and allows for more rotation and uniform ductility demands in the components of the structures. However, plastic hinges at the bottom of the columns are almost unavoidable (see Fig. 1b).

While the design standards for steel-RC ensure satisfactory performance of the three components of MRF (beams, columns, joints) under earthquake loads, the long-term performance of these structures can be compromised by potential steel corrosion [9,10]. Corrosion problems can lead to the loss of stiffness and complete failure of the structures. Additionally, the costs of repair and maintenance due to corrosion are significant [11], accounting for 2.5 trillion dollars annually on a global scale, as reported in 2013 [12]. Epoxy coatings have been shown to partially safeguard steel bars from corrosion [13,14]. Nevertheless, the long-term degradation of epoxy coatings is unavoidable, which could result in more severe corrosion of the steel bars [15].

Many efforts have been made to replace steel reinforcement with noncorrodible alternatives. In particular, fibre-reinforced polymer (FRP) bars have garnered significant attention. FRPs are manufactured by using fibres embedded in a resin matrix. The mechanical properties of FRPs are mainly governed by the fibres, while the resin facilitates stress transfer and distribution between fibres [11], [16]. Commonly used fibres include carbon, aramid, basalt, and glass [16], and depending on the type of fibre, the properties of the FRP reinforcements vary. Regardless of types of fibre, FRP composite material offers an excellent alternative to steel due to its benefits including high strength-to-weight ratio, ease of installation, and good durability [17], [18].

Among various types of FRP materials, Glass Fibre Reinforced Polymers (GFRP) are less expensive, and offer high strength, thermal stability, and durability [19] making them more attractive to the construction industry. GFRP can be used as external reinforcement to strengthen existing buildings [20–22] or as effective internal reinforcement, especially in sever environmental conditions [23,24] i.e. structures in marine environment, jetties, water bridges, waste water treatment facilities and region with high humidity, salts or chloride exposure. These conditions significantly accelerate the corrosion of conventional steel reinforcement, leading to reduced service life, increased maintenance costs, and potential structural failure. The high strength-to-weight ratio of GFRP facilities the ease handling and placement of reinforcement in these critical structures especially those located in the harsh environments. Therefore, GFRP reinforcement offer a high effective alternative in these applications due to these exceptional properties, extending the service life of the structure and reduce the life cycle maintenance cost.

The mechanical and physical properties of GFRP, such as the low modulus of elasticity, and shear strength, as well as bond behaviour, are significantly different from those of steel [25]. Steel reinforcement behaves in an elastic-plastic manner, exhibiting ductile behaviour with a modulus of elasticity approximately three times that of GFRP. In contrast, GFRP behaves linearly elastic up to failure, making it more brittle compared to the ductile behaviour characteristic of steel. Due to the low modulus of elasticity of GFRP, flexural members reinforced with GFRP exhibit wider cracks and larger deflections than their steel-reinforced counterparts [26]. Therefore, the design of GFRP-RC members is normally governed by the serviceability limit state [26–28]. It has also been reported that the lower stiffness of GFRP than steel can potentially cause column instability problems [29]. Additionally, the bond performance of GFRP reinforcement in concrete is a critical parameter to achieve a desirable load transfer mechanism [30].

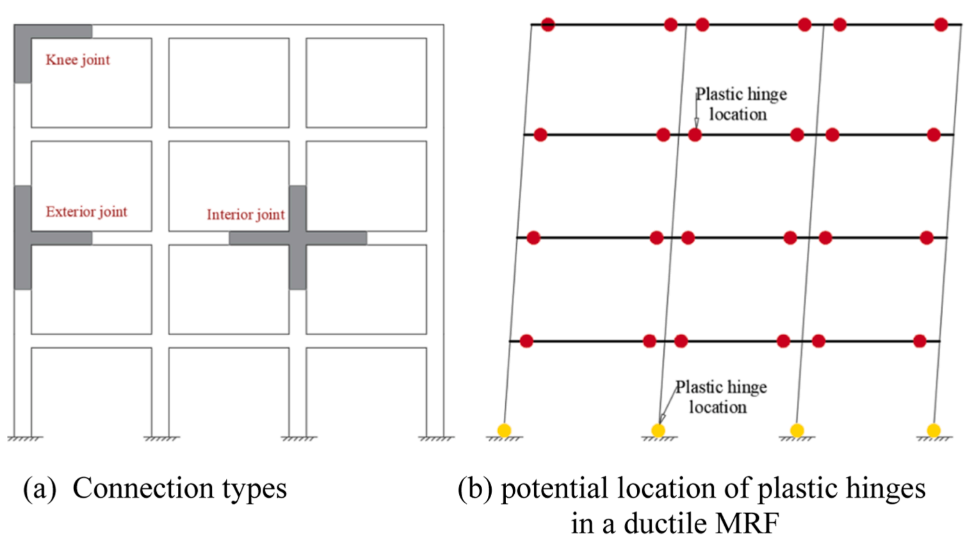

Fig. 1. Moment resisting frame.

Surface treatment of GFRP bars using sand coating and surface deformation showed its efficiency in improving bond strength [31–33]. Owing to sufficient research on GFRP-RC elements in the last couple of decades, the design of GFRP-RC individual elements under flexural, axial and shear forces is now well-reflected in established standards [34].

The flexural design philosophy of GFRP-RC elements differs from that of steel-RC elements. Steel-RC flexural members are usually designed as tension-controlled (under-reinforced) elements, with failure controlled by bar yielding, whereas GFRP-RC members are commonly designed as compression-controlled (over-reinforced) elements where failure is initiated by concrete crushing prior to the bars' rupture. Compression-controlled failure is preferred over tension-controlled failure in GFRP-RC due to the linear elastic behaviour of GFRP bars up to tension failure [35]. The unique combination of high tensile strength and low modulus of elasticity of GFRP bars enable GFRP-RC structures to endure high deformations before failure, often providing warnings of impending failure. However, as the failure is governed by bar rupture or concrete crushing, the ductility and energy dissipation of such structures are lower than the conventional steel-RC counterparts. Large reduction factors of 0.55 for tension-controlled design and 0.65 for compression-controlled design are adopted in the ACI 440.11–22 design standard [34] to ensure the same level of reliability as in steel-RC structures. It is worth noting that the ductility of compression-controlled failure can be enhanced by ensuring adequate confinement to the concrete or by using more ductile concrete materials such as fibre-reinforced or high-performance concrete [36]. This raises questions about the use of the constant strength reduction factor of 0.65 for all compression-controlled failure scenarios.

The existing GFRP-RC design standard ACI 440.11–22 does not incorporate seismic design considerations [34]. Particularly under seismic loads, the performance of MRF poses a significant challenge due to the linear elastic behaviour of GFRP, which can adversely affect its ductility and ability to dissipate earthquake loads. Tests of individual elements such as columns [37], walls [38], and slabs [39] with GFRP reinforcement under earthquake-simulated load demonstrated the applicability of GFRP-RC to be used under seismic loads. The feasibility of using GFRP in columns under cyclic loads has been demonstrated, highlighting its ability to reach high deformation levels with no strength degradation [37]. Improved cyclic performance of GFRP-RC columns was achieved with the use of ultra-high-performance concrete [40]. The design of MRF in seismic regions should achieve adequate ductility to effectively dissipate seismic loads. Therefore, the feasibility of using GFRP in MRF is questionable. Its low modulus of elasticity can result in excessive deformation of structures under earthquake loads, subsequently increasing the contribution of the P-Δ effect. Understanding the behaviour of GFRP-RC MRF under seismic loads is essential to ensure its widespread application.

In the last few decades, the behaviour of GFRP-RC beam-column sub-assemblages have garnered attention in research due to its critical structural role [41–44]. To understand the performance of the connection to promote the applicability of GFRP-RC MRFs in seismic regions, a comprehensive literature review study is conducted to gain insights into the proper design of these critical regions. The general behaviour of GFRP-RC concrete connections is discussed and compared to that of steel-RC counterparts. The seismic performance, in terms of ductility, stiffness, energy dissipation, and damage, is critically discussed and the key differences with the steel-RC counterparts are highlighted. Various parameters affecting the performance of the connection are identified, analysed and presented in an in-depth discussion. For the completeness of the study, the paper provides a straightforward perspective of current issues related to seismic performance of GFRP-RC MRFs as well as pointing out the gaps regarding the better understanding of GFRP-RC MRFs performance and guiding the future research toward establishing seismic provisions for GFRP-RC MRFs.

2. Seismic performance comparison of MRFs reinforced with steel and GFRP bars

Japanese researchers began investigating the feasibility of using FRP reinforcement in RC MRFs under simulated earthquake loads [45]. Their experimental study on multi-story MRF reinforced with aramid fibre-reinforced polymers (AFRP) proved that MRFs FRP-RC can withstand seismic loads. The tests of beam-column sub-assemblages under simulated seismic loads also confirmed that carbon fibre polymer (CFRP) was a suitable alternative for steel reinforcement [46]. Research on the applicability of GFRP in MRFs showed an adequate performance in terms of strength and deformability of beam-column sub-assemblages using longitudinal and grid GFRP transverse reinforcement (see Fig. 2a) [47]. GFRP stirrups #13 and spaced 100 mm, in the form of two C-channels forming rectangular stirrups, were also employed (see Fig. 2b) [41]. It was found that such GFRP-RC beam-column sub-assemblages can attain the design capacity and sustain cyclic loads without degradation of the strength of the bars. Subsequent sections will discuss the seismic performance of connections in MRFs reinforced with GFRP and evaluate the effect of several parameters affecting its response.

2.1. Failure mode and hysteresis behaviour

The investigations on the performance of GFRP-RC MRFs began by evaluating the seismic response of exterior beam-column connections with GFRP in comparison to conventional steel reinforcement [41,42]. In terms of crack development, initial cracks formed in the beam adjacent to the column and then increased with the application of load for both reinforcement options. Unlike steel, where cracks in the beam concentrated in the zone adjacent to the column (see Fig. 3a), cracks in the GFRP extended along a larger length of the beam and almost closed after each loading step. A virtual plastic hinge developed away from the column, spreading over a larger area compared to the concentrated plastic hinge observed in steel due to local yielding (see Fig. 3b) [41].

The hysteresis response of beam-column connections with GFRP and steel reinforcement is completely different. The GFRP-RC beam-column sub-assemblages showed a linear response with narrow hysteresis loops, while steel-reinforced specimens exhibited wide hysteresis loops (see Fig. 4). Up to the maximum applied drift of 5 %, the GFRP-RC specimen showed no strength degradation. In another study, GFRP-RC beam-column sub-assemblages were able to reach a drift ratio of more than 6.5 % [42]. Hence, the performance was deemed acceptable in terms of drift demand. Compared to the steel-RC connection, the specimen with GFRP exhibited larger shear deformations in the joint panel. This subsequently increased the contribution of joint deformation to the total deformation in the case of GFRP, adding significantly to the overall deformation of the frame [42]. It was concluded that GFRP is suitable for use in beam-column sub-assemblages with the ability to resist compression and tension cycles. Therefore, such structures can be designed to satisfy both strength and deformation requirements with the capability of sustaining at least a 4 % drift [41].

The performance of interior beam-column sub-assemblages was also evaluated [43] where it was shown that up to a drift ratio of 5.5 %, the GFRP-RC specimen did not exhibit any brittle damage, indicating that the specimens can withstand larger deformation. Further study on 3D interior connections with lateral beams confirmed that the connections were able to reach 8 % drift without experiencing brittle failure [44]. Although GFRP-RC beam-column sub-assemblages attained their design capacity, the rate of load increase was slow with increasing the drift ratio [43]. Interestingly it was found that steel-RC specimens showed a rapid decrease in capacity after the peak load, while that in GFRP-RC connections decreased slowly [43]. This demonstrates the pseudo-ductile performance of GFRP-RC, highlighting its potential use in seismic regions.

Story drift is usually controlled to prevent damage to non-structural

(a) Grid transverse reinforcement [47] (b) C-channels transverse reinforcement [41]

Fig. 2. Early employed GFRP in connections.

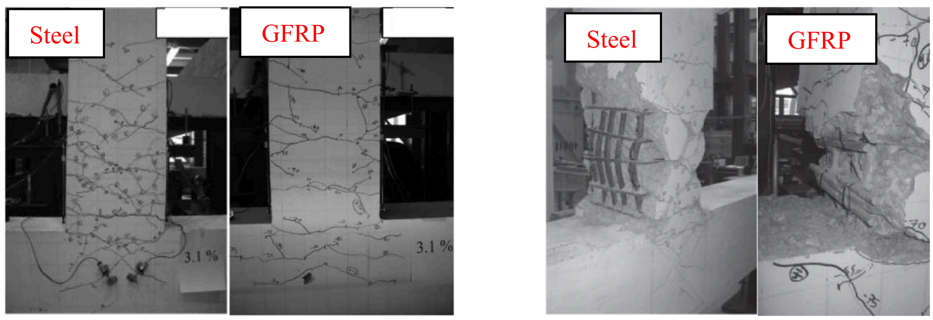

(a) Cracks propagation (b) Specimens at failure

Fig. 3. Early employed GFRP in connections [41].

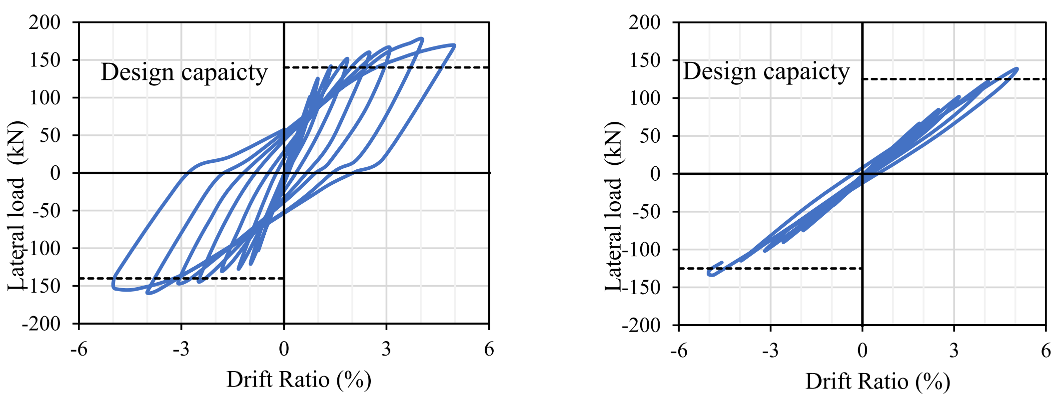

(a) Steel reinforcement (b) GFRP reinforcement

Fig. 4. Hysteresis behaviour of steel and GFRP-RC connections [42].

elements. It should be noted that, according to [48], deformable GFRP-RC MRFs is designed to withstand a minimum drift ratio of 4 %. However, according to [49,50], the allowable story drift for RC MRFs is 2.5 %. From the discussed results, it seems that GFRP-reinforced structures usually reach their design capacity at greater drifts. This means that at a small level of drifts i.e., 2.5 %, the full capacity of the GFRP-RC structure may not necessarily be reached which needs to be considered in design. The analysis of tests on beam-column connection from different studies indicated that at 2.5 % drift, 49–91 % of the capacity can be achieved. A value of about 75 % of the design capacity is considered the most probable value. Meanwhile, at 4 % drift, the average achieved capacity was about 89 %, as shown in Fig. 5b. These observations are significantly different from those of steel-reinforced frames, where almost all test results for control specimens (see Fig. 5a) achieved their design capacity prior to 2.5 % drift. Hence, it seems that depending on the design drift and stiffness of the system, a reduced capacity of GFRP-RC MRFs of about 75 % of the target capacity should be considered to meet the design criteria for avoiding damage to non-structural elements.

While GFRP material is characterised by linear elastic up to failure, the experimental observations showed gradual failure rather than brittle failure [44]. This is mainly due to the less brittle compression-controlled failure of GFRP-RC elements at the farthest compression fibres with the loss of concrete cover near the joint. It was found that even at this point the damage remained limited to unconfined concrete cover [44]. Additionally, the effect of confinement by stirrups improved the contribution of the core concrete, and the specimens continued to gain higher capacity after the loss of concrete cover [44]. Although the failure of GFRP-RC may not be as ductile as steel yielding in steel-RC, there is a level of ductility especially if the concrete is effectively confined. This once again shows that GFRP-RC MRFs can potentially be designed to provide a level of ductility. Especially with the use of fibre-reinforced concrete or ultra-high-performance concrete, the compression-controlled mechanism can be improved and accordingly,

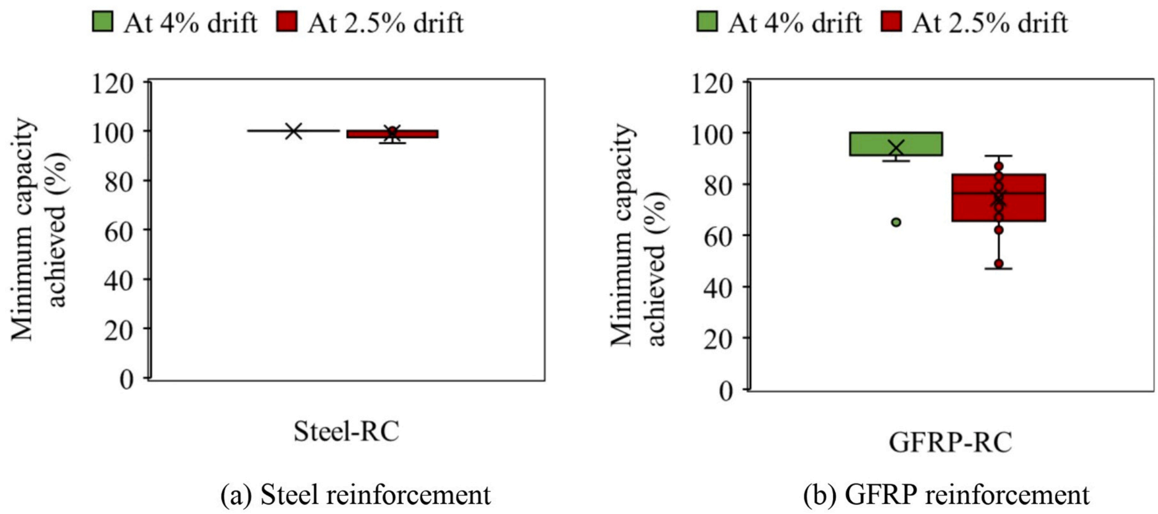

Fig. 5. Capacity analysis of steel and GFRP-RC connections.

partially enhance the ductility [36,40].

2.2. Reinforcement strains

Examining the reinforcement strains is essential for understanding the behaviour of RC members. Differences were reported between strain development in both steel and GFRP-RC connections. In comparison to steel, where the strain of steel reinforcement suddenly increased, GFRP-RC specimens exhibited slow growth of the strain of GFRP without a sudden increase, resulting in lower strains compared to steel-RC [43]. As reported by [41], the residual strains in connections subjected to large drifts were different between steel and GFRP-RC connections. It was reported that after 4 % drift, longitudinal GFRP reinforcement exhibited negligible residual strain compared to the permanent plastic strains in steel-RC connections [41]. This indicates that, during a strong earthquake, GFRP-RC MRF remains functional with minimal damage that requires minimal repair due to its linear elastic behaviour. It was also reported in [43] that the strains of the hoops at the joint core for steel were greater than those of GFRP indicating that the joint with steel reinforcement experienced more severe damage due to excessive plastic deformations and hence higher joint shear forces [43]. According to [44], a significant margin between reinforcement strain and its rupture strain should be achieved to ensure gradual damage without brittle failure. Hence, strains should be checked during the design of sections to ensure a safe margin [44]. It should be noted that concrete damage can affect the theoretical calculation of the strains by increasing the stress in the reinforcement. However, as found in [44], the difference in strain between measured and theoretical calculations was only about three percent. A margin of 40 % between the capacity and expected stress was suggested to prevent brittle rupture failure and ensure gradual failure, as reported in [51]. Therefore, it should be checked that the stress in GFRP reinforcement is limited to a percentage of its strength to avoid the risk of brittle failure under earthquakes. However, more studies are required to define the optimum considered percentage of bar strength to provide both a safe and cost-effective design.

2.3. Residual damage

Residual damage is a critical parameter indicating the functionality of structures after earthquake. GFRP-RC beam-column connections have been shown to exhibit significantly lower residual displacements compared to those of steel, increasing the functionality of the structure after cyclic loads [43,44]. This reduction in damage has the potential to lower post-earthquake retrofit and rehabilitation costs. On the other hand, the yielding of steel reinforcement during cyclic loads prevents the structure from returning to its original conditions [44], which results in extra repair costs. This indicates that the GFRP-RC structures exhibits stronger self-centring behaviour than steel ones due to the linear elastic behaviour of GFRP. To investigate its behaviour after repeated loads, the GFRP-RC connections were retested [44]. The GFRP-RC specimen was able to reach its design capacity again and reinforcement strains was almost the same as the values obtained in the first loading cycle [44]. However, due to existing damage from the first loading, the stiffness was reduced, design capacity was attained at a higher drift ratio, and the connections exhibited a linear response up to the peak load [44]. While no decrease in lateral load was found in the first loading, the second loading showed a decrease in lateral load after reaching the peak (see Fig. 6) due to excessive damage [44]. This points to the potential ability of GFRP-RC MRFs to withstand multiple earthquakes loads with minimal damage, thus potentially lowering maintenance costs.

2.4. Stiffness deterioration

Stiffness deterioration is an important indicator of the cumulative damage caused by earthquake loads. Previous studies showed that the initial stiffness of steel-RC beam-column sub-assemblage was higher than that of GFRP-RC ones due to the reduced modulus of elasticity [41, 52]. As reported in [53], the initial stiffness of GFRP-RC beam-column sub-assemblages exhibited a 70 % reduction compared to the steel-RC counterpart. However, the rate of stiffness degradation is greater in steel-RC compared to GFRP-RC. It has also been reported that the stiffness at a 4 % drift of the steel-RC specimens was 70 % of its initial stiffness, while the degradation of the GFRP-RC ones was not significant (see Fig. 7a) [41]. This observation is in line with another study where at a 4 % drift ratio, the loss of stiffness was as low as 22 % of its initial stiffness for the GFRP-RC specimens while this degradation was more significant at about 65 % of its initial stiffness in the case of steel-RC ones [52]. The rapid rate of stiffness deterioration in steel-RC connections is due to the excessive damage caused by plastic deformations as a result of steel reinforcement yielding [43,54]. Since GFRP does not exhibit any yield, the sources of stiffness degradation are mainly concrete cracking, cover spalling, and reinforcement slippage [55]. The reduced initial stiffness of GFRP-RC connections was also confirmed in [44]. However, a higher flexural reinforcement ratio was found to control the percentage of reduction [44].

The reduced stiffness of the GFRP-RC connections results in increased deformations, and subsequently, the effect of the secondary moment can potentially become relatively considerable. This secondary

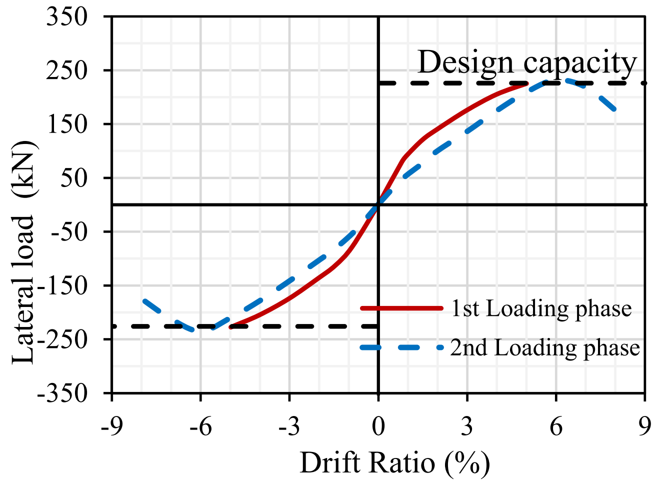

Fig. 6. Effect of repeated earthquakes loads on GFRP-RC structures [44].

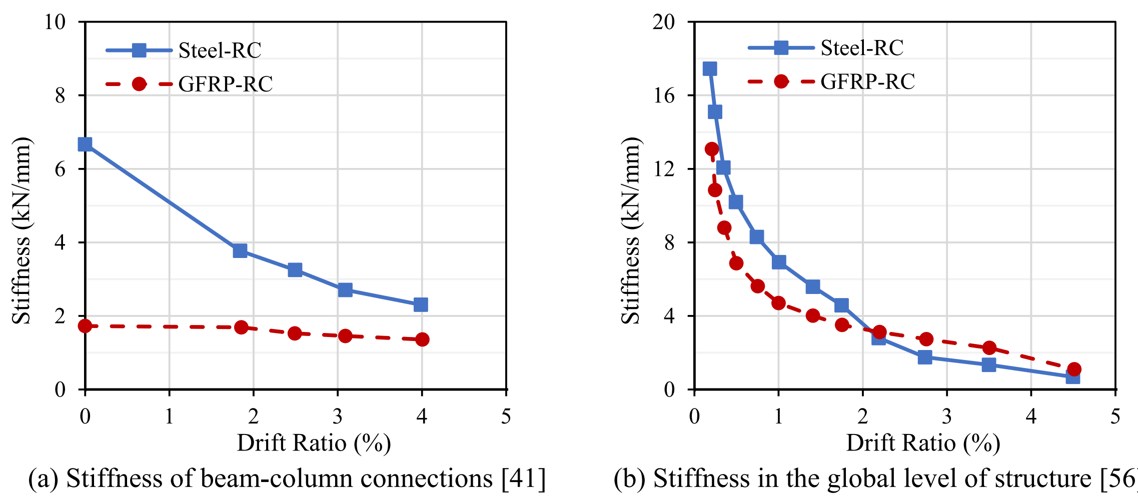

Fig. 7. Comparison of stiffness in steel and GFRP-RC structures.

moment increases the moments acting on the end of the column, increasing the risk of column failure before the beam [44]. It was reported that, the secondary moment can cause the column capacity to be exceeded at a 4 % drift. The quantification of this increase indicated that the secondary moment can significantly increase the moment applied to the column by about 19 % at a 5 % drift [51]. Thus, they concluded that the drift of GFRP-MRFRs should be limited to 4 % [51].

Different trends were reported on the global scale of the structure (Full MRF). While the initial stiffness of steel-RC MRFs was higher than that of GFRP-RC MRFs by around 31 %, the stiffness at around 2.2 % drift became the same due to the higher degradation of stiffness in the steel one, attributed to bar yielding (see Fig. 7b) [56]. In another study focused on the seismic performance under push-over analysis of multi-story frames, it was shown that the initial stiffness of the GFRP-RC MRFs was less than that of steel by 21 % and 18 % for the case of five and three-story frames, respectively [57]. On the other hand, according to [58], it was reported that the reduced stiffness attracts lower forces under earthquake loads with the cost of increased displacement. Therefore, the total base shear of the structure is less due to the increased natural period of the structures, which, in turn, reduces the design ground acceleration [58]. Further studies are required at the global scale of structures to further understand the stiffness degradation of GFRP-RC MRFs under earthquakes.

2.5. *Energy dissipation*

The energy dissipation capacity is a critical parameter in the seismic design of structures. Structures with higher energy dissipation capacity can effectively dissipate the input energy from earthquakes. To compare the energy dissipation capacity of systems, the area under hysteresis loops is usually considered. Steel-RC connections exhibit larger loop areas due to plastic deformations [43]. The plastic deformations due to steel yielding, concrete inelastic deformation due to cracking and crashing, and reinforcement slippage are the main components contributes to dissipates the energy. The ductile response of steel-RC enhances energy dissipation during high drift, with significant deformations and increased bar slippage after yielding [43]. Yielding of steel is the main source of energy dissipation in steel-RC while plastic deformations and slippage have little contribution [42]. Due to the elastic behaviour of GFRP bars, in GFRP-RC the hysteresis loops are generally narrower which indicating a relatively lower energy dissipation capacity. Despite GFRP being brittle, GFRP-RC connections still possess some energy dissipation [43] primarily from inelastic concrete deformation and concrete damage [59] as well as bar slippage [55]. The level of concrete damage due to joint distortion, which is controlled by the joint reinforcement details and well confinement concrete delaying the spalling, as well as the anchorage performance affecting the slippage, both determine the level of dissipated energy.

A previous study reported that steel-RC beam-column sub-assemblages dissipate overall energy four times higher than that with GFRP reinforcement [42]. Another study reported that GFRP-RC beam-column sub-assemblages showed a 50 % reduction in energy dissipation compared to steel ones at the same drift ratio [43]. In a third study, the steel-RC beam-column sub-assemblage was reported to exhibit five times higher energy dissipation than GFRP at a drift of 2.5 %, which then increased to more than six times at 4 % drift (see Fig. 8a) [41]. According to [44] the energy dissipation capacity of GFRP-RC connections was enhanced by increasing the level of shear stress applied to the joint which caused increased damage to the joint and significant slippage. This increased level of joint shear, due to a higher beam reinforcement ratio, improved the energy dissipation by a greater contribution of concrete in the compression zone due to a larger height of the compression zone [59]. This in turn increased the contribution of the inelastic behaviour of concrete and led to increased dissipated energy [52]. Additionally, when the failure mode changes from beam balanced failure to concrete crushing failure with good confinement to the joint by GFRP stirrups, causing the delay of spalling, the energy dissipating capacity of GFRP-RC can be enhanced to be only one-third of that with steel reinforcement at a drift ratio of 2.5 % [52] compared to the five times reported in [41]. These reasons explain the reported different levels of dissipated energy among studies. Overall, steel-RC beam-column sub-assemblages showed higher energy dissipation capacity, between three to five times that with GFRP, depending on the observed damage, the possibility of bar slippage of GFRP, and the failure mode.

Tests on the global scale showed a closer difference in the dissipated energy between steel and GFRP-RC MRFs. It was found that on average steel-RC MRFs had a 49 % higher energy dissipation capacity than GFRP-RC MRFs at about 2.5 % drift [56]. This once again indicates the much enhanced energy dissipation at the global level of structure which was limited to half of that in steel-RC MRF compared to the previously mentioned value of one-third of that with steel reinforcement at a drift ratio of 2.5 % reported in [52]. This again is attributed to the larger contribution of inelastic deformation of concrete, increased concrete damage at different parts of the global structure, and concrete confinement. The same study also confirmed the critical role of confining the concrete at the joint region. A considerable increase of 50 % in the dissipated energy at 2.5 % drift was observed by confining the joint region by transverse links compared to an identical unconfined GFRP-RC MRF [52]. Interestingly, both steel and GFRP-RC frames were reported to achieve the same energy dissipation when the drift ratio approached 4 % (see Fig. 8b) [56].. However, steel stirrups were used as transverse reinforcement and the effect of axial load was discarded, which could affect the damage evolution and impact the findings [56]. Regarding the use of steel stirrups, it was confirmed in another study that the energy dissipation of GFRP-RC beam-column sub-assemblages with GFRP stirrups is comparable to that with steel stirrups [52]. When considering the energy dissipation capacity of GFRP-RC, two points need to be considered. Firstly, even though GFRP bars are elastic, GFRP-RC exhibits inelastic behaviour. By improving the ductility of concrete material, the level of energy dissipation can be increased. Secondly, at the structural level, the overall energy dissipation of GFRP-RC MRFs is not significantly lower than that of steel-RC MRFs and is sometimes comparable. Further studies on these aspects are recommended to better understand the energy dissipation capacity of GFRP-RC.

2.6. Ductility

Ductility is the ability of the element to sustain inelastic deformations before failure without substantial loss of strength. It is a critical aspect in MRFs which are expected to undergo inelastic deformations under seismic loads. Ductility can be expressed in terms of inelastic energy absorption or deformations [60]. In the first approach, higher inelastic energy absorption is preferred to mitigate the elastic brittle catastrophic failure. In the latter, the structural member should be able to undergo greater deformations along with wide cracks before failure [60]. Due to the brittle linear elastic response of GFRP reinforcement, the ductility of structures reinforced with GFRP is questionable. However, research [58] claimed that due to the large deformations of structures reinforced with GFRP, these structures can be designed to achieve deformation capacity and acceptable deformability, replacing the ductility of steel-RC structures.

For evaluating the ductility of GFRP-RC MRFs, attention should be given to the inherent differences between the behaviour of steel and GFRP. Hence, the common methods used for steel-RC may not be applicable to GFRP-RC. The displacement ductility factor is usually used to quantify the ductility [62] which for steel-RC is defined as the ultimate displacement divided by the yield point displacement. One of the common methods proposed by Park [61] to determine these points is shown in Fig. 9 as an example. As shown, the ultimate displacement Δ_u is considered at the point where the load is dropped by 20 %. This assumption is valid for steel-reinforced structures since the cycle loops are wide and stable, reasonably reflecting the dissipated energy represented by the area under the load-displacement envelope. The

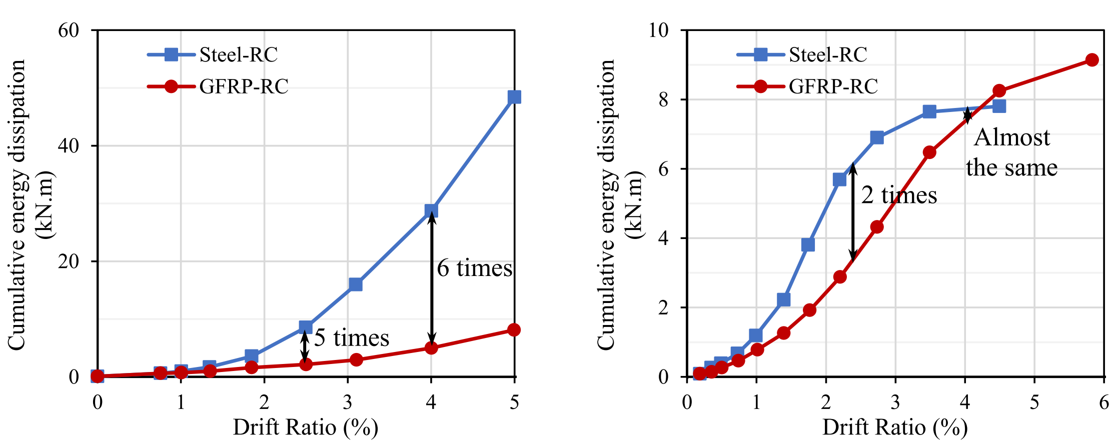

(a) Energy dissipation of beam-column connections [41]
(b) Energy dissipation in the global level of structure [56]

Fig. 8. Comparison of energy dissipation in steel and GFRP-RC structures.

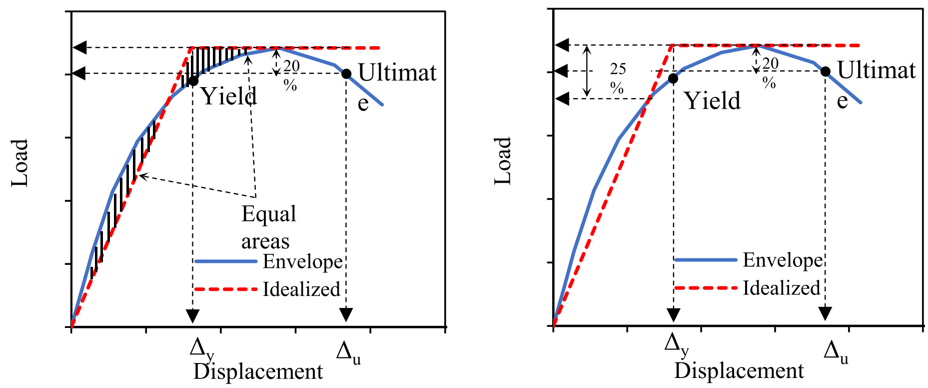

Fig. 9. Methods for ductility calculation for steel structures [61].

displacement at yield point Δ_y can be calculated either based on equivalent elasto-plastic energy absorption concept or reduced stiffness equivalent elasto plastic yield [61]. Since both common methods were developed based on elasto-plastic yield, extending these methods to GFRP is questionable since GFRP does not yield [39]. These approaches led to obtaining higher values of displacement ductility factor when applied to GFRP-RC columns under cyclic load [63].

Ductility definition as the ratio between ultimate deformation to the yield deformation is not suitable for GFRP-RC members due to the lack of yielding point. Although previous research has addressed this point [65,66], there is no solid definition of ductility of GFRP-RC members [60]. Different methods have been proposed to determine the ductility of GFRP-RC structures. Due to the linear elastic behaviour of GFRP, a real plastic hinge is not present, and virtual plastic hinges are usually used to describe the part of the connection where large elastic deformations of the bars occur. A deformability-based approach known as the J-factor was proposed, which considers the increased moment and deformations in beams [67]. In structures with a perfect elastic response up to failure, the J-factor represents the ratio of stored energy at failure to that when the concrete strain reaches 0.001 [67]. Despite the satisfactory performance of GFRP-RC in terms of deformation, most of the energy is elastic. Because inelastic energy dissipation is an essential property for ductility of structures, an energy-based approach was suggested by [68]. In this approach, the ductility index is simply represented by the ratio between inelastic energy and total energy. Other research [39] and [64] suggested that a virtual elastic displacement Δ_e can be considered as the transition between elastic and inelastic behaviour instead of the yield displacement Δ_y. Under cyclic loads, research [64] and [39] suggested that this point can be defined at the intersection between the secant stiffness line passing through the service load P_s and the horizontal line passing through the peak load P_u (see Fig. 10a). While according to [38], this virtual transition point is experimentally defined at the point where the structure starts to lose its self-centring behaviour, which is indicated by cracks no longer closing and not realigning during unloading with permanent deformations. Kharal [69] claimed that this point can be obtained when the difference of the tangential slope at the origin and at the secant slope is greater than 15 %. Because GFRP-RC connections mostly did not show any strength degradation up to the peak load, the ultimate displacement at the peak load was suggested to be considered as Δ_u [64]. Another method based on the equivalent energy elastic-plastic (EEEP) bilinear idealization method was suggested to define the ultimate and elastic displacement [38]. In this method, the ultimate point was estimated as the point resulting in equal areas, as shown in Fig. 10b, with the suggestion of limiting Δ_u to the maximum drift ratio $\Delta_{capacity}$ of 2.5 % as the maximum ultimate drift. Clearly, the estimation of ductility for GFRP-RC is varied in the literature, subject to simplifications and assumptions, and lacks a solid definition

A comparison of displacement ductility factor for both GFRP and steel-RC connection was reported at different scales. According to the method followed in [64], the GFRP-RC connection achieved a displacement ductility factor greater than 2. However, it was about 72–86 % of that of steel ones, depending on the well-detailing of the connection reinforcement [64]. In pushover analysis of GFRP-RC multistorey frames [57], it was found that the drift of the global MRF was comparable to counterpart steel-RC MRF. In addition, the GFRP-RC MRFs performed satisfactorily in terms of ductility and strength. However, the three-story MRFs provided higher ductility compared to the five-story frame [57]. This indicates that the GFRP-RC MRFs satisfy acceptable ductility.

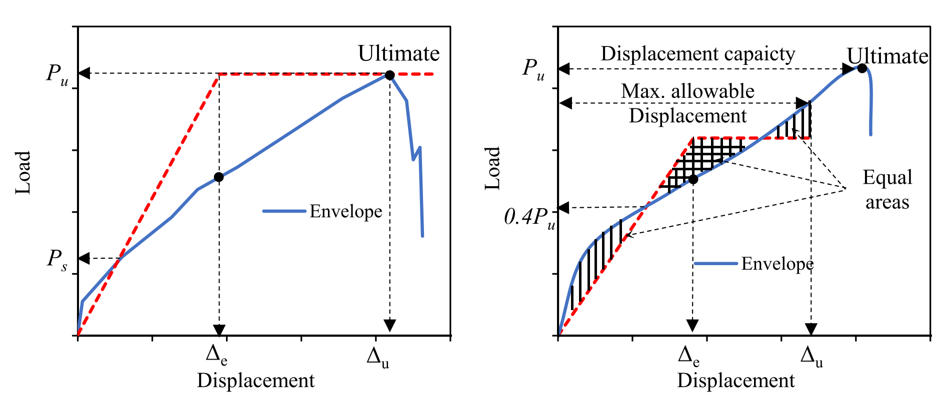

Fig. 10. Proposed methods for calculating the ductility of GFRP-RC structures.

3. The balance between advantages and challenges in seismic design of GFRP-RC structures

Adequate lateral deformation is a critical criterion for the performance of RC structures, particularly in terms of ductility and energy dissipation. It has been shown that, although GFRP reinforcement does not exhibit yielding, it stands out due to its unique combination of a low modulus of elasticity and high tensile strength compared to other FRP materials. This enables GFRP-RC members to undergo significant deformations, enhancing their deformability. As demonstrated in the previous sections, these structures achieved a minimum drift ratio of 4 %. This behaviour contrasts with CFRP-RC, which, despite its higher tensile strength, is less capable of undergoing substantial deformations.

On the other hand, larger deformations in GFRP-RC structures pose structural challenges. Increased joint deformations can reduce the stiffness of the structure, potentially leading to a soft-story mechanism and collapse, while also damaging non-structural elements. As such, serviceability limit states become a critical design consideration for GFRP-RC structures. Furthermore, greater lateral deformations increase the second-order effects, particularly the $P-\Delta$ effect, which increases column moments and may shift the failure mode to column failure—an undesirable and catastrophic failure mode in MRFs. Therefore, the design of GFRP-RC MRFs should balance the benefits of GFRP's unique properties while mitigating failure risks.

While story drift is usually controlled to mitigate these challenges, the analysis of tested specimens shown in Fig. 5 indicates that when the maximum allowable drift ratio of 2.5 % for conventional RC structures is applied, the full capacity of GFRP-MRFs may not be realized, which needs to be considered in design. The analysis results, as mentioned, indicated that at 2.5 % drift, 75 % of the design capacity is considered the most probable value. These observations are significantly different from those of steel-reinforced frames, where almost all test results showed that steel-RC specimens achieved their design capacity prior to 2.5 % drift. Hence, it seems that by controlling the design drift, a reduced capacity of GFRP-RC MRFs, about 75 % of the target capacity, should be considered to meet the design criteria for avoiding the risks of excessive lateral deformations.

4. Parameters affecting the connection response

4.1. Influence of beam to column flexural capacity

Most design codes for steel-RC require that the column-to-beam flexural capacity ratio should be greater than 1 to ensure the strong column weak beam concept [5–7]. Previous studies on GFRP-RC experimentally evaluated the influence of this ratio [44,59]. The first study [59] examined the variation of this ratio from 1.21 to 1.92. In the other study, the influence of the flexural ratio between 0.83 and 1.16 was evaluated [44]. A lower flexural ratio of 0.83 caused the column to reach its capacity prior to the beam, where concrete spalling of the column was observed [44]. Subsequently, this led to decreased lateral stiffness, and the design capacity was not achieved. With the least beam reinforcement ratio, the failure was mainly due to concrete cracking and crushing at the beam, with minor cracks at the joint region due to low shear stress acting on the joint (see Fig. 11a) [59]. The further increase in the beam reinforcement ratio led to more crack observations at the joint due to higher shear forces acting on the joint region and caused more damage [44,59]. The joint region suffered severe X-shaped cracks due to the high introduced shear stress to the joint that led to more spalling of concrete (see Fig. 11b) [59]. Crushing of concrete was also observed at the column since the flexural ratio was reduced. It was reported that, a higher beam reinforcement ratio can change the failure from the beam to the undesired joint shear failure [59]. Therefore, the beam reinforcement ratio should be limited by the joint shear capacity as long as the strong column weak beam concept is achieved.

The beam reinforcement ratio has a double side effect. While research [59] suggested to keep the beam reinforcement ratio as low as 0.7 % to ensure that beam-column sub-assemblages fail in beam flexure, a lower beam reinforcement ratio is risky. This can increase the possibility of bar rupture, causing a brittle and catastrophic failure [70]. The bar rupture failure in knee connections changed to diagonal concrete failure with an increase in the reinforcement ratio from 0.38 % and 0.86–1.29 % [70]. Another study suggested providing a well-over-reinforced beam ratio to ensure gradual failure and avoid bar rupture [52]. It should be noted that beams are usually designed with GFRP reinforcement between 1.5 and 2.5 times the balanced reinforcement to meet serviceability requirements. This range can ensure the elimination of brittle failure [52]. As mentioned previously, secondary moments in GFRP-RC MRFs due to reduced stiffness increase the acting moments on the column [51]. However, it was found that with the consideration of secondary moments, the failure still occurred in the beam in the case of a flexural ratio of 1.16 [44]. These outcomes confirm that the suggested ratio of 1.2 for flexural ratio according to the design codes is still applicable [5–7]. However, this conclusion was confirmed only for an axial load ratio of 0.15 and may need further examination under a wide range of higher column loads. The applicability of the suggested ratio of 1.2 under higher axial loads needs to be further examined.

4.2. Effect of concrete compressive strength

Concrete strength plays an essential role in determining the response of GFRP-RC structures. The effect of different concrete strengths, on the response of exterior beam-column sub-assemblages [71] and interior beam-column sub-assemblages [43] was evaluated. It was found that the joint shear strength and initial stiffness increased with increasing concrete strength [43,71]. Additionally, flexural reinforcement strains increased with higher concrete strength, contributing to a higher shear force at the joint region [43]. A comparison at the same level of joint shear stress was conducted for concrete strengths of 30 MPa and 70 MPa [72]. The mode of failure for both specimens was similar. However, with a concrete strength of 30 MPa, the peak capacity was obtained at 4 % drift, while it was obtained at 5 % drift in the case of 70 MPa. [72]. The degradation of strength was observed at an earlier drift ratio in low concrete strength than in the high strength of 70 MPa [72]. Another study [44] theoretically investigated the effect of concrete strength ranging from 20 to 80 MPa. It was highlighted that for GFRP-RC beam-column sub-assemblages, the relation between the square root

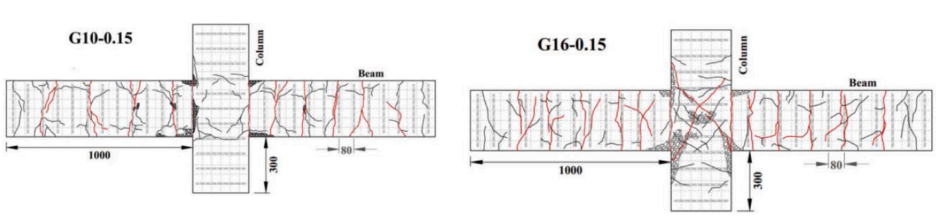

(a) Failure with low beam reinforcement ratio

(b) Failure with high beam reinforcement ratio

Fig. 11. Influence of beam reinforcement ratio of GFRP-RC MRF [59].

of concrete strength and the acting joint shear stress is approximately linear. This was different from the trend in steel-reinforced connections, which followed a decelerating increase relation (see Fig. 12) [44].

Special types of concrete can maximize the benefits of the high strength-to-weight ratio of GFRP. For example, an improved capacity of 25 % was obtained by replacing traditional concrete with a strength of 32 MPa in conventional steel-reinforced connections by lightweight concrete with a strength of 42 MPa, along with GFRP bars with the same reinforcement amount [73]. Additionally, adding steel fibres to lightweight concrete further increased the capacity as well as improved the deformability of connections with GFRP reinforcement [73]. However, steel fibres do not provide corrosion-free structures as the efficiency of steel fibres can be diminished in harsh environments [74,75]. Self-consolidating concrete can be of high efficiency due to the congestion of reinforcement at the connection [76]. Specimen made with self-consolidating concrete of strength 45 MPa not only showed improved capacity but also had improved stiffness compared to concrete with a strength of 30 MPa [76]. While special types of concrete have shown promising benefits, studies employing ductile concrete in connections of GFRP-RC MRFs like ultra-high-performance concrete (UHPC) and engineering cementitious composite (ECC) are still needed.

4.3. Effect of joint reinforcement

Joint reinforcement is essential to achieve the joint capacity. Previous studies have demonstrated the efficiency of GFRP joint stirrups in improving connection capacity [71,77]. As reported in [77], the inclusion of joint stirrups increased the connection capacity by 17 %. Although the progression of failure was quite similar to the connection without stirrups, diagonal shear cracks were initiated at the joint core at drifts of 2.5 % and 3 % without and with joint stirrups, respectively [77]. The connection without stirrups exhibited an obvious pinching effect, while the presence of stirrups alleviated this effect [77]. In another study, due to the lack of seismic provisions for GFRP-RC MRFs, the required GFRP joint stirrups were provided according to seismic requirements for steel-RC MRFs [44]. The tested connections performed satisfactorily up to 5 % drift without damage to the connection region, and none of the stirrups reached their ultimate strain [44]. A numerical study revealed a linear increase in connection capacity with increasing the amount of joint reinforcement [78]. However, it was observed that the performance of the connection remained unchanged when the joint reinforcement ratio exceeded 0.6 % [78]. To further fill this gap, researchers are encouraged to explicitly evaluate the effect of joint stirrups and their spacing on joint capacity. This suggestion is aligned with conclusions drawn from studies on steel-RC structures, where joint stirrups were considered as tension ties and crack control reinforcement rather than confining reinforcement [79]. Considering this, analytical models for steel-RC structures explicitly take into account the effect of joint shear reinforcement [80,81]. Moreover, it has been reported that the efficacy of joint stirrups in steel-RC structures depends on their location, with stirrups placed in the middle working more effectively [82].

Different forms of joint reinforcement can be utilized. For example, the use of spiral reinforcement at the joint core resulted in no significant damage, indicating its effective application [43]. An enhancement in the peak load and the energy dissipation was observed with increasing the diameter of confining spiral reinforcement [43]. In knee joints, it is essential to provide joint reinforcement in the form of a mesh in two directions. However, due to the manufacturing constraints of GFRP stirrups, the construction of mesh options might be challenging. An alternative suggestion is to use diagonal stirrups to confine the joint region [70]. The proposed details, as shown in Fig. 13a, resulted in achieving 7 % higher capacity than the design capacity, while the unconfined connection achieved only 66 % of the design capacity [70]. These observations affirm the effective contribution of the inclined reinforcement in controlling the widening of the formed shear cracks with and without chamfers. However, the inclusion of chamfer and inclined reinforcement provided a stiffer and stronger connection due to the additional contribution of concrete at the interior corner, avoiding brittle failure [70]. The use of X-shaped reinforced with reduced horizontal stirrups, as shown in Fig. 13b, led to a higher capacity of 5 % than conventional GFRP stirrups [83]. The X-shaped reinforcement demonstrated its ability to resist diagonal tension and control the shear cracks at the joint region [83].

Innovative non-conventional confinement option was also proposed. An internal FRP tube was proposed to properly confine the joint core and mitigate the problem of reinforcement congestion caused by the stirrups at the joint (see Fig. 13c) [77]. Diagonal cracks at the joint region appeared at a delayed drift compared to that with conventional stirrups. However, the connection with tubes of large thickness suffered extended cracks outside of the joint core due to severe spalling of the concrete cover. This led to its separation from internal concrete and subsequently impacted the obtained capacity negatively [77]. Tubes with fibres oriented at a 45-degree angle showed superior performance in terms of controlled concrete spalling and improved capacity by 30 % with wider hysteresis loops [77]. The improved response is attributed to the effectiveness of inclined fibres at 45 degrees in restraining the opening of shear cracks in the principal stress direction. A significant improvement

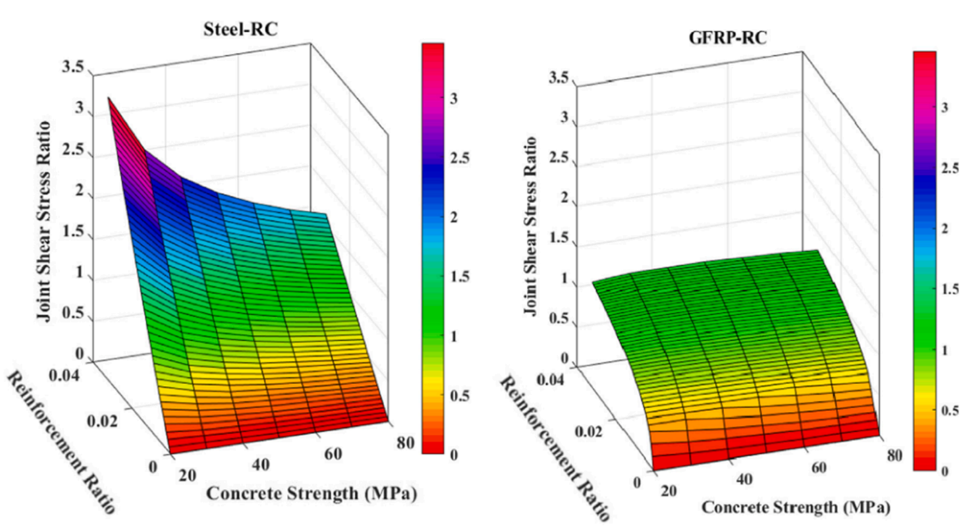

Fig. 12. Effect of concrete strength on both steel and GFRP-RC structures [44].

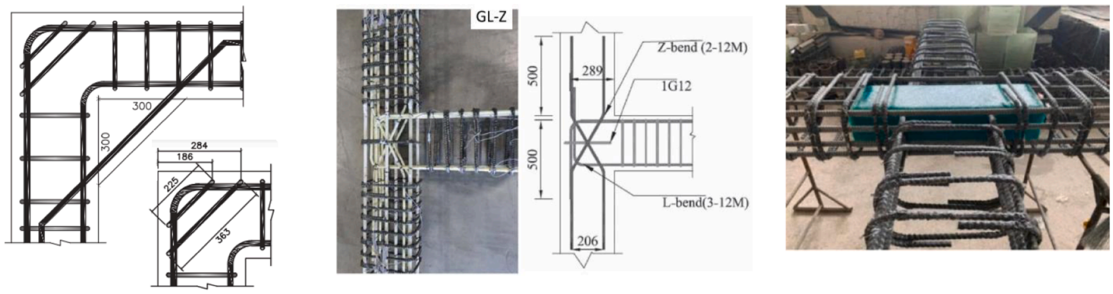

(a) Inclined confinement to knee joints [70]   (b) X-shape reinforcement [83]   (c) Tube confinement [77]

Fig. 13. Connection details for the joint region of GFRP-RC MRF.

in energy dissipation was obtained after a drift ratio of 3 %, where shear cracks became more prominent [77].

4.4. Effect of anchorage detailing

The problem of anchorage is more critical in knee and exterior connections than in interior connections due to the limited space to accommodate the required anchorage length. Adequate embedded length inside the joint region should be provided to ensure the proper transfer of forces. Since the column size is generally small, a common practice is to use 90-degree bent bars [7]. The poor anchorage can lead to a sudden drop in strength, reducing the ductility of the structures under cyclic loads [84]. Slippage of bars causes a sudden increase in the bar stress, which in turn can lead to bar rupture. Especially with GFRP, this becomes more critical due to the reduced strength at the bends, which can reach 55 % of the straight bars [85]. These problems were confirmed in knee connections tested by [70] which failed in a brittle catastrophic manner due to bar rupture at the onset of the bend, achieving only 64 % of the design capacity.

Different straight anchorage lengths can affect the connection's response. For example, the connection with straight bars of 20 times the bar diameter (20d) failed due to slippage at an earlier drift while the connection with a larger embedded length of 30d failed due to concrete crushing followed by bar rupture after approaching the target capacity [86]. Therefore, it was concluded that an anchorage length of 30d is enough to prevent slippage failure [86]. In a subsequent study, the anchorage length of 24d and 30d was evaluated with the aim of finding the optimum length. It was found that the anchorage length of 24d was adequate to prevent slippage failure [52].

Different options can be used for proper anchorage. For example, connection with hooked bars achieved a higher capacity by 26 % compared to that with straight bars with embedded lengths equal to 20d, which failed due to slippage [58]. However, the full target capacity was not achieved with the hooked bars [58]. As a second option, the use of a beam stub to terminate the straight beam bars approximately achieved the full design capacity with a beam failure [58]. In other studies, the use of steel-hooked couplers for anchorage [71,87] demonstrated an improved connection capacity. It was also reported that sand-coated bars led to improved capacity than grooved and threaded surfaces due to proper bond conditions [71]. Compared to steel-reinforced connections, the capacity of the connection with sand-coated surfaces was higher by 5 %. While other bars led to a reduced capacity by 10 % compared to steel [71]. Headed bars, on the other hand, have potential benefits in avoiding the reduced strength at the bends and alleviating reinforcement congestion at the joint. It was found that exterior beam-column connections with headed bar anchorage were able to withstand drifts of up to 4 % without strength degradation [88]. It was also reported that in the case of deformed bar surfaces, there was a sudden drop in strength at a drift of 4.6 % due to slippage resulting from bearing failure at the anchorage head [88]. While sand-coated bars were able to resist loads up to 6 % drift.

A comparison between the response of connections with headed bars and bent bars anchorage was carried out. As found in [88], connections with bent bars were able to sustain larger drifts than headed bars with a stable gradual degradation of strength. This is due to the additional confinement added to the joint region by the bent tail. It was also found that deformed bars achieved greater excess capacity than sand-coated bars despite the earlier failure of deformed bars compared to sand-coated ones [88]. Despite the difference between the two options, both connections were able to attain the maximum capacity, demonstrating that headed bars are comparable to bent bars [88]. In another study [54], connections with headed bars exhibited stable behaviour without joint damage up to a drift ratio of 4 %. Both bent bars and headed bars connections showed the same linear behaviour up to 6 % drift [54]. However, bent bars can prevent the movement of the bars inside the joint and provide more favourable confinement by the tail during reversal loading at high drifts [54]. The effect of bent bars on the connection capacity becomes evident when the joint is subjected to high shear stresses. Finally, it was concluded that the anchorage performance of both headed bars and bent bars is generally the same up to a drift ratio of 4 %.

Innovative connection detailing can further improve its performance. In standard 90-degree hook anchorage, the tail length of the hook should be at least 12d according to [34] to ensure proper force transfer within the joint. It was found that the connection capacity using a tail length of 37d was improved by 40 % compared to the case with a tail length of 16d [83]. The results are in agreement with [89], where the capacity of conventional steel-reinforced exterior connections depended on the provided tail length [89]. However, the degree of enhancement of the connection due to the tail length increase also depended on the available column thickness [89]. While a 40 % increase in capacity was demonstrated, the larger tail length was used along with diagonal bars connecting the beam to the column (see Fig. 14) [83]. These additional inclined bars alone proved to have a high contribution in improving the steel-reinforced connection performance with the potential to reduce the amount of connection confinement [82]. In a subsequent study [64], the use of U-shaped bars (see Fig. 14b) for anchoring the beam bars (beam top bars connected to bottom bars as one unit) along with the same inclined bars at the connection corners was also compared with the standard hook. The same level of improvement achieved with longer L bars was also achieved with typical detailing with U-shaped anchorage [64]. This confirms that the improvement in connection performance may be attributed to the inclusion of additional corner bars, which can add additional resistance to the beam longitudinal bars. Otherwise, both U and L bars are believed to achieve the same performance. However, it is worth mentioning that extensive research on conventional steel-RC joints confirmed that U-shaped bars resulted in reduced capacity compared to those with L bars [81,90,91]. Therefore, further research is required to quantify the contribution of each tail length and additional inclined bars.

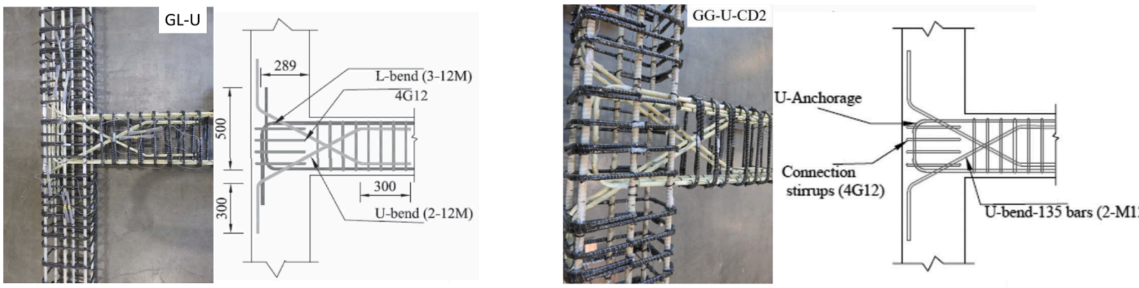

(a) Increased tail length (b) U bars

Fig. 14. Anchored bars with additional diagonal bars [83].

4.5. Effect of column axial load

Column axial load is a critical parameter that governs the response of beam-column connections. As reported in [43], increasing the axial load from 0.1 to 0.3 of the column axial capacity reduced both the maximum load and deformations. The reduction in deformability reflected its negative impact on connection ductility [43]. As the applied column load increased from 0.1 to 0.2, the maximum load was reduced by 25 %, and this reduction reached 41 % and 50 % with a further increase in the applied load ratio to 0.25 and 0.3, respectively. On the other hand, higher column loads led to improved dissipation of energy by enhancing aggregate interlocking, while the rate of stiffness deterioration and residual deformations increased [43].

Experimental tests with higher axial loads can present challenges due to the limited capacity of hydraulic jacks and the large size of test specimens. Therefore, numerical investigations have investigated a wide range of axial loads. It was also found that higher column axial load degrades the beam-column sub-assemblage performance causing the inability of specimens to achieve its design capacity even with good confinement to the joint with lateral beams [92]. However, with 75 % of the column capacity as a high axial load, the effect of joint shear stress level was less pronounced [92]. In another study, it was concluded that increasing the column axial load ratio from 10 % to 60 % led to a 36 % reduction in the capacity [93]. This reduction is attributed to the increased compression stress at the joint region, which can be further increased by applying the beam load. This caused the beam to fail due to reaching the concrete compressive strain in the compression area because of the compression-controlled design. In a subsequent study, [94], it was found that the degradation due to an axial load can be controlled by using X-shaped reinforcement in the joint region. While columns in real structures are subjected to different axial load levels, such axial load effects should be considered in the design of beam-column joints. It should be noted that such effects in GFRP-RC beam-column sub-assemblages are different from the two-sided effects effectively considered in predicting the joint shear strength of steel ones [95].

4.6. Effect of joint aspect ratio

The joint aspect ratio is defined as the ratio between the beam thickness to the column thickness. Despite its critical impact on joint shear strength, the effect of joint aspect ratio has been studied superficially with most research was carried out on specimens with a joint aspect ratio of 1.0 [44,59,77]. Results from [71] confirmed that the joint shear strength was reduced with an increasing joint aspect ratio from 1.0 to 1.33. The effect of a joint aspect ratio between 0.88 and 1.4 was also numerically investigated by changing the column thickness while keeping the beam size unchanged [93]. The results, as shown in Fig. 15, indicated that the maximum load decreased as the joint aspect ratio increased. While this increase in capacity can be attributed to the increased joint area offered by the increased column cross-section, a more comprehensive comparison can be obtained by changing the beam size as long as the beam does not fail before the joint. A connection with a high aspect ratio requires an increased number of stirrups to properly confine the developed steeper strut mechanism in the joint region. This can be more critical than in steel since GFRP stirrups have low transverse strength and stiffness, which may affect their efficiency. Therefore, in-depth studies are recommended to better understand the behaviour of connections with a high aspect ratio.

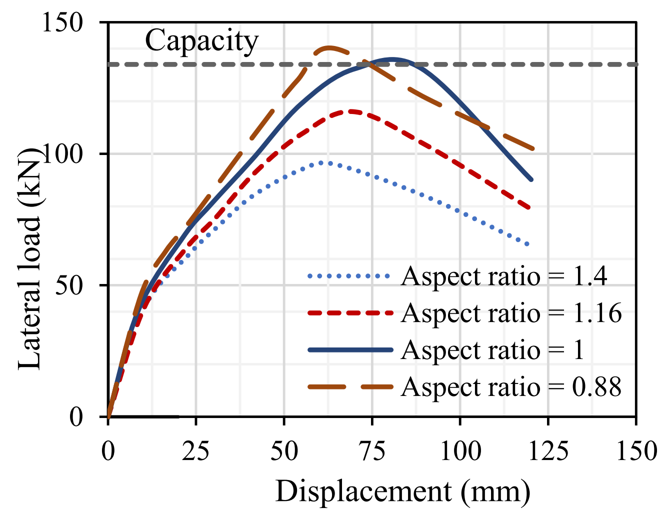

Fig. 15. Effect of joint aspect ratio on the capacity of GFRP-RC connection [93].

4.7. Effect of the presence of floor slab

The interaction of the floor slab with the beams can change the flexural ratio between the column and beam. The floor slab can potentially increase the beam flexural capacity and, therefore, increase the risk of column failure instead of beam failure, which contradicts the concept of a weak beam and a strong column [96]. In addition, neglecting the presence of the slab can lead to an underestimation of the lateral stiffness, which, in turn, can lead to an overestimation of the lateral deformation of GFRP-RC MRFs. Theoretically, because GFRP-RC sections are mostly designed as compression-controlled, the effective flange width of the slab in compression could reduce the reinforcement ratio and change the compression failure of concrete to the undesirable brittle rupture of the GFRP bar. This is significantly different from steel, where the failure of steel is ductile, and the mode of failure does not change.

Effective slab width can be estimated considering the equivalent length of the slab that could be represented by the maximum strain in beam reinforcement. In a previous study [96], it was found that the contribution of the slab to increase the capacity of interior beam-column connection was more pronounced in steel-RC connections than in GFRP-RC. The increase of capacity was 36 % for the steel-RC connection compared to 10 % for GFRP-RC. Additionally, connections with a slab exhibited more damage penetration to the joint than those without a slab, due to reducing the ratio between beam and column flexural capacity [96]. The effective flange width for steel-RC connections was found to be 2 times the beam depth, while it is limited to 1.2 times the beam depth in GFRP-RC connections [96]. This is attributed to the low modulus of elasticity causing increased deflection of the slab in the transverse direction. Different from theoretical considerations, the results revealed that the slab in compression for GFRP-RC did not affect the beam flexural capacity [96]. For the slab acting in tension, the theoretical expected bending capacity was not achieved; however, an increase in the flexural capacity was obtained. This observation was different from the case with steel reinforcement, where the slab in tension was more pronounced in increasing the capacity, and both the slab in tension and compression approached their theoretical design value [96]. In the subsequent numerical modelling, it was found that the effective slab width depends on the available width of the slab. This trend was demonstrated in both steel-RC and GFRP-RC [96].

The effect of the slab in exterior beam-column connection differs from interior connections due to unsymmetrical geometry. In such cases, slab loads generate torsional cracks at the lateral beams. Similar to interior connections, the test results on exterior connections contradict concerns about the presence of the slab in compression, showing a minor effect on the capacity [55]. The effective width of the slab was found to be 0.85d and 0.5d with and without lateral beams, respectively [55]. In terms of crack propagation, exterior connections exhibited a clear propagation of torsional cracks in the lateral beams due to the beam bars' forces (see Fig. 16a) [55]. Such torsional cracks were not observed in interior connections (see Fig. 16b) [96].

The presence of the slab significantly increased the initial stiffness of the beam-column subassemblies. However, the degradation of stiffness was more noticeable with the presence of a slab than in specimens without slabs [55]. To avoid the reduction in stiffness, it was suggested to limit the drift ratio to 3 % [55]. The presence of slab also led to a significant improvement in the energy dissipation capacity. At a drift of 5 %, an improvement in energy dissipation by 122 % and 49 % was obtained for specimens with slab and without lateral beams and slab with lateral beams, respectively [55]. At a lower drift ratio of 3 %, the improvement percentages were 145 % and 89 %, respectively. It is worth mentioning that the energy dissipation of tested slabs with GFRP in the first cycle was closer to a similar slab with steel reinforcement under cyclic load [97]. Clearly, the contribution of the slab in a real structure should be considered to avoid the underestimated performance of MRFs.

4.8. Effect of transverse beams

The presence of lateral beams can improve the performance of beam-column sub-assemblages due to the better confinement they offer. As reported in [54], connections without lateral beams showed a lower lateral capacity compared to those with lateral beams [54]. At a drift ratio of 6 %, connections without lateral beams suffered significant concrete expansion at the joint area accompanied by a drop in strength [54]. According to [55], the presence of lateral beams in exterior connections resulted in wider hysteresis loops, increased stiffness and improved capacity due to proper confinement to the joint (see Fig. 17a), which subsequently led to more energy dissipation due to damage occurring in a large volume of concrete. In addition, specimens without transverse beams suffered significant penetration of the damage compared to those with lateral beams. Moreover, the presence of lateral beams in exterior beam-column connections improved the contribution of the slab in tension to the moment capacity. As shown in Fig. 17b, an increase in capacity by 30 % was observed with the presence of the slab, compared to Fig. 17a, while the contribution of the slab was less pronounced in cases without beams [55].

The size of lateral beams determines their efficiency. It was numerically found that increasing the size of lateral beams improved the connection capacity and reduced the damage at the joint, subsequently reducing the shear stress transferred to the joint stirrups [92]. This contribution of lateral beams was more significant in cases where the joint was subjected to higher joint shear stress. With low shear stress, joint expansion became insignificant, leading to less efficiency of lateral beams in offering confinement to improve joint shear strength [92]. It was also found that the contribution of the slab increases with increasing the size of the transverse beams due to improving the contribution of slab rebars [55,96].

5. Strength prediction of beam-column joint

The joint shear strength estimated based on two approaches. The first is the strut mechanism, where the forces are transferred within the joint through a wide strut, with the joint reinforcement acting as confining reinforcement. The second is the truss mechanism, where the forces are transferred through multiple struts, and the joint reinforcement functions as tension ties. The strut mechanism is adopted in most steel-RC design standards for joint shear strength is described in terms of concrete strength as $\gamma\sqrt{f_c'}$ [5,7]. The factor γ is determined based on the

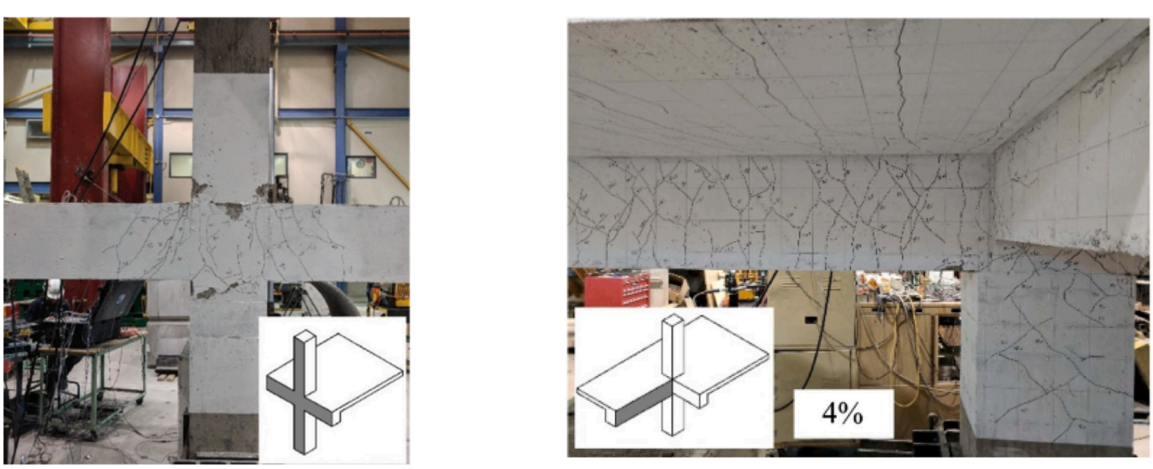

(a) Exterior connection [55] (b) Interior connection [96].

Fig. 16. Crack behaviour in transverse beams.

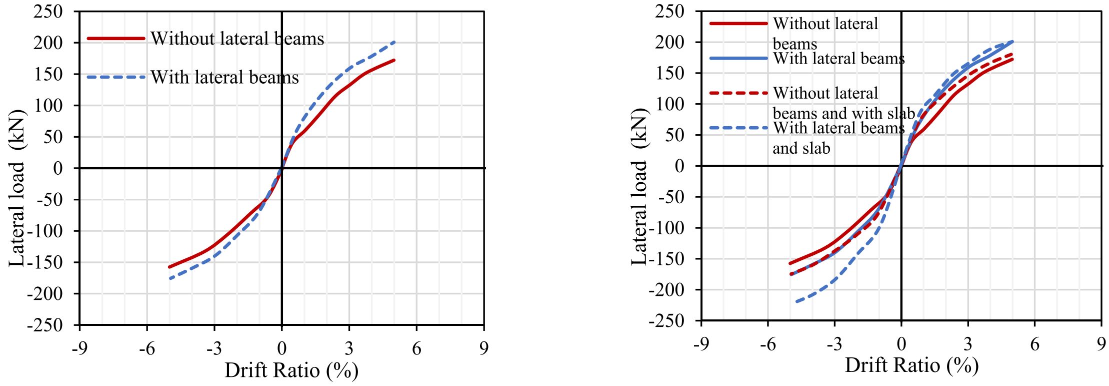

(a) Without slab

(b) With slab and without slab

Fig. 17. Effect of lateral beams [55].

level of confinement provided by lateral beams. Sufficient joint shear reinforcement should be provided to ensure joint capacity. However, this approach to determining the joint capacity is based on strut mechanisms, where the amount of joint reinforcement, joint aspect ratio, and axial load are disregarded. On the other hand, CSA 2012 [48] does not provide a limit to joint shear strength. Thus, higher shear forces applied to the joint can lead to a catastrophic joint shear failure.

To determine the joint capacity, the effect of different levels of shear stress acting on the exterior joint was investigated [72]. The joint region was confined by stirrups according to the provisions for columns as per CSA 2002 [98]. Three modes of failure were observed, as shown in Fig. 18. With a low shear stress of $0.7\sqrt{f_c'}$, the specimen failed due to the beam flexure. A sudden reduction in strength was observed once the capacity was achieved due to the high stress in the bars causing slippage. Under the other two shear stress levels, a gradual degradation of strength was observed. The shear stress of $0.85\sqrt{f_c'}$ changed the mode of failure from beam flexural failure to simultaneous beam and joint failure. The last failure mode with shear stress of $1.0\sqrt{f_c'}$ was joint shear failure with severe cracks at the joint region extending to the column sides accompanied by the loss of concrete cover. According to their observations, it was suggested that the joint shear strength of exterior connections should be limited to $0.85\sqrt{f_c'}$ to avoid undesired failure modes [72].

When it comes to exterior beam-column connection with lateral beams, the shear stress level of $0.85\sqrt{f_c'}$ resulted in brittle failure due to beam bar rupture accompanied by bar slippage [54]. While the mode of failure of specimen subjected to a shear stress of 1.1 $\sqrt{f_c'}$ was accompanied by beam and joint cracks. In a subsequent study [51], additional specimens were tested under shear stress of $1.3\sqrt{f_c'}$ to examine their ability to withstand higher shear stress ratios. The results indicated that exterior beam-column connections were also able to maintain their capacity under shear stress of $1.3\sqrt{f_c'}$ [51] when the seismic provisions for columns are satisfied according to CSA 2017 [99]. Although the exterior connection exhibited severe damage to the joint region, an identical interior connection under the same joint shear stress level was intact and exhibited more residual deformations than exterior ones with a low rate of stiffness degradation due to the proper confinement [51]. To determine the capacity of interior beam-column connections with lateral beams, other tests were conducted [44]. The connection was able to resist shear stress up to $1.8\sqrt{f_c'}$ [44]. However, the capacity of interior connections without lateral beams still has not been covered. These conclusions were basically developed for a specific joint aspect ratio, the amount of joint stirrup, and axial load. This capacity can further be affected by the ignored parameters. Such parameters were effectively considered in the prediction of joint shear strength of steel-reinforced structures [4,80,81]. Future studies can consider these parameters for proposing an accurate formula to predict the joint shear capacity.

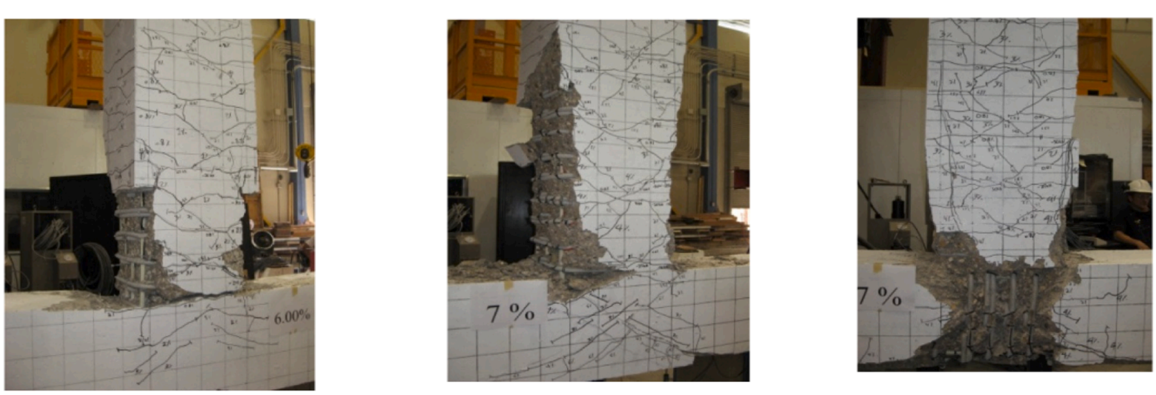

(a) Beam failure (b) Beam and joint failure (c) Joint failure

Fig. 18. Effect of joint shear stress on the observed mode of failure [72].

6. Joint structural analysis and failure prediction

The highlighted portion of the frame structure in Fig. 1a between the points of contraflexure is used for the structural analysis of the beam-column joint. Generally, three criteria are essential for the design of beam-column connections in RC-MRFs. However, as previously noted, the provisions for GFRP-RC connections in existing GFRP design standards are limited or absent. This section integrates the fundamentals of these well-known criteria, the outcomes highlighted in this study, and the available design guidelines for GFRP-RC sections to support the analysis and design of GFRP-RC connections.

According to ACI 352–02 [5], the first criterion for the design of connections is that the column's flexural capacity should be at least 20 % greater than the beam's flexural capacity. This ensures that the plastic hinge forms in the beam rather than in the column. The results discussed in this study confirm that the same criterion is applicable to GFRP-RC beam-column connections. However, as previously noted, this ratio requires further investigation under conditions of high axial loads. The nominal flexural capacity of columns and beams for the GFRP-RC section M_n can be determined according to the design provisions available in design standards for GFRP-RC based on internal force equilibrium and strain compatibility, Eq. (1).

$$M_n = A_f f_r \left[d - \frac{a}{2} \right] \tag{1}$$

Where d is the effective depth, a is the depth of equivalent stress block, A_f is the tensile reinforcement area, f_r is the tensile stress in the GFRP which is limited to the design tensile strength of GFRP f_{fu}, Eq. (2).

$$f_{fu} = C_E f^*_{fu} \tag{2}$$

Where C_E is an environmental reduction factor, taken as 0.85 according to ACI 440.11–22 [34]. In contrast, its value is specified as 0.7 for concrete exposed to earth or weather and 0.8 for unexposed concrete, as per ACI 440.1R-15 [25], AASHTO [100] and Italian CNR [101]. Other design standards, such as Canadian CSA [48] and Japanese JSCE [102] do not account for the environmental reduction factor and therefore consider it equal to 1.0.

The forces and moments from the beam and column are transferred to the joint region as joint shear forces V_{jh}, as shown in Fig. 19. The horizontal joint shear force V_{jh} can be determined according to Eq. (3) for the interior, and Eq. (4) for the exterior connections, respectively. If the applied joint shear force V_{jh} exceeds the joint shear capacity V_n, a joint shear failure governs the structure failure. Otherwise, a flexural beam failure is expected, provided that the first design criterion is met. The nominal joint shear capacity V_n is calculated using Eq. (5). Therefore, the second design criterion is to ensure that the applied joint shear force V_{jh} is less than the joint shear capacity V_n to prevent catastrophic joint failure.

$$V_{jh} = T_1 + T_2 - V_{col} \tag{3}$$

$$V_{jh} = T_1 - V_{col} \tag{4}$$

$$V_n = v_n A_j \tag{5}$$

Where T_1 : is the tensile force in the reinforcement at the top of the beam, T_2 : Tensile force in the reinforcement at the bottom of the beam. V_{col} : the column shear force, v_n : is the maximum allowable joint shear stress, A_j is the joint sectional area and is equal to $b_j \times h_c$ where b_j is the joint width and h_c is the column depth in the analysis direction.

Currently, there is no established formula in the design standard that provides provisions for the joint shear capacity of GFRP-RC beam-column joints. However, based on this review paper and as highlighted in the previous sections, exterior connections without lateral beams should be limited to $0.85\sqrt{f'_c}$, exterior connections confined by lateral beams to $1.3\sqrt{f'_c}$, and interior connections confined by lateral beams to $1.8\sqrt{f'_c}$. It is important to note that joint shear capacity depends on the connection's location and the presence of confining beams in standard design guidelines for steel-RC connections. For instance, according to [5], the joint shear strength for exterior connections without lateral beams in steel-RC is $1.0\sqrt{f'_c}$, increasing to $1.25\sqrt{f'_c}$ and $1.66\sqrt{f'_c}$ for exterior and interior connections confined by lateral beams, respectively. The suggested values for GFRP-RC connections differ from those for

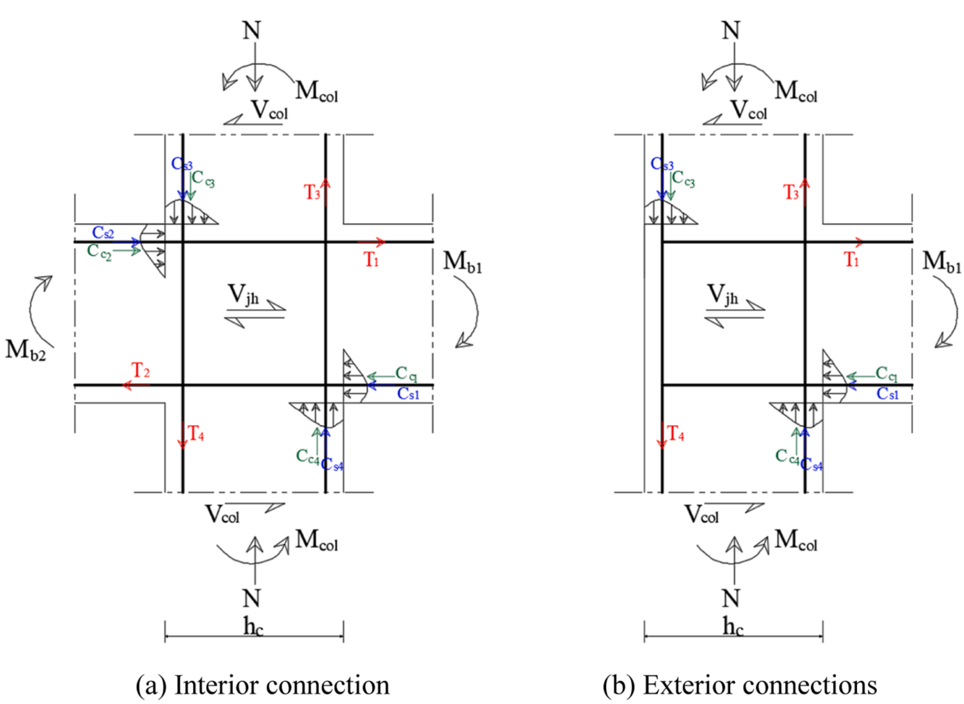

Fig. 19. Internal forces at the joint region.

conventional steel-RC connections due to differences in behaviour. However, the trend aligns with the outcomes of this study, where the joint shear strength changes with changing the connection configuration, highlighting the need for further research into other configurations, such as interior connections without lateral beams and knee joints, to address these gaps.

The third criterion in the design of beam-column joints is to provide minimum confinement reinforcement in the joint region to ensure an effective force transfer mechanism and achieve the desired design strength. However, guidelines for this minimum reinforcement are absent in GFRP-RC standards, leaving it as an open research topic to determine the minimum confinement required to meet the recommended strength values.

7. Advancements in using GFRP in different MRFs systems

Recent research suggested techniques to improve the low-energy dissipation of GFRP-RC MRFs. The energy due to ground motion consists of potential, kinematic, damping, and hysteresis energy. The first two components vanish once the static equilibrium of the structure is achieved. Thus, damping and hysteresis components become crucial. When significant inelastic deformation occurs, the hysteresis component increases. While GFRP-RC structures exhibit a low hysteresis damping component, these structures need to be designed with a damping component. External damping components in the form of supplementary rebar systems [103], inclined demountable wall systems [104], replaceable steel fuses [105] proved its efficiency in improving the energy dissipation capacity of structures with self-centring behaviour. Another approach to address this main drawback is the use of hybrid systems, in which the structure can be designed with steel for post-peak response [42]. Previous research suggested that a hybrid structural system can be utilized at the global structure, where external MRFs are reinforced with GFRP to prevent corrosion [54]. Steel-reinforced systems, like shear walls, can be used inside the building to improve its energy dissipation. Hybrid reinforcement was also able to improve the energy dissipation capacity [106]. However, both hybrid systems or reinforcement may lead to a decline in the benefits of GFRP to eliminate corrosion and permanent deformation, which cause difficulties in rehabilitation due to steel yielding.

Implementing an additional damping system can be an effective solution to enhance the dissipation of earthquake energy of GFRP-RC MRFs. An easy-to-install damping system was proposed in [107] (see Fig. 20a). The proposed system utilized external steel plates attached to the beams of the MRF. The system was designed to benefit from the absence of permanent deformation in GFRP while incorporating the high energy dissipation capacity of steel. The steel plates were externally attached to the beams, making them physically accessible and replaceable after yielding while ensuring minimal damage to the main structure. The results demonstrated that the new system exhibited higher capacity compared to a GFRP-RC one. Additionally, the initial stiffness of the system was almost equal to a structure reinforced with steel. The energy dissipation capacity was improved by 160 % at a 2.5 % drift compared to the basic GFRP-RC structure. However, it was found that the proposed system still dissipates energy less than steel-reinforced structures [107]. The steel plates deformed significantly, and after their removal, the structure approximately returned to its original condition. Tests conducted after replacing the plates confirmed the acceptable performance of the structure (see Fig. 20d). It should be noted that the main objective was to improve seismic performance rather than achieving corrosion-free structures. However, the suggested system prevents the internal corrosion, which is difficult to access for repair. Therefore, stainless steel components can be used to address the issue of external corrosion, ensuring superior structural performance.

On another note, since GFRP-reinforced structures have a low

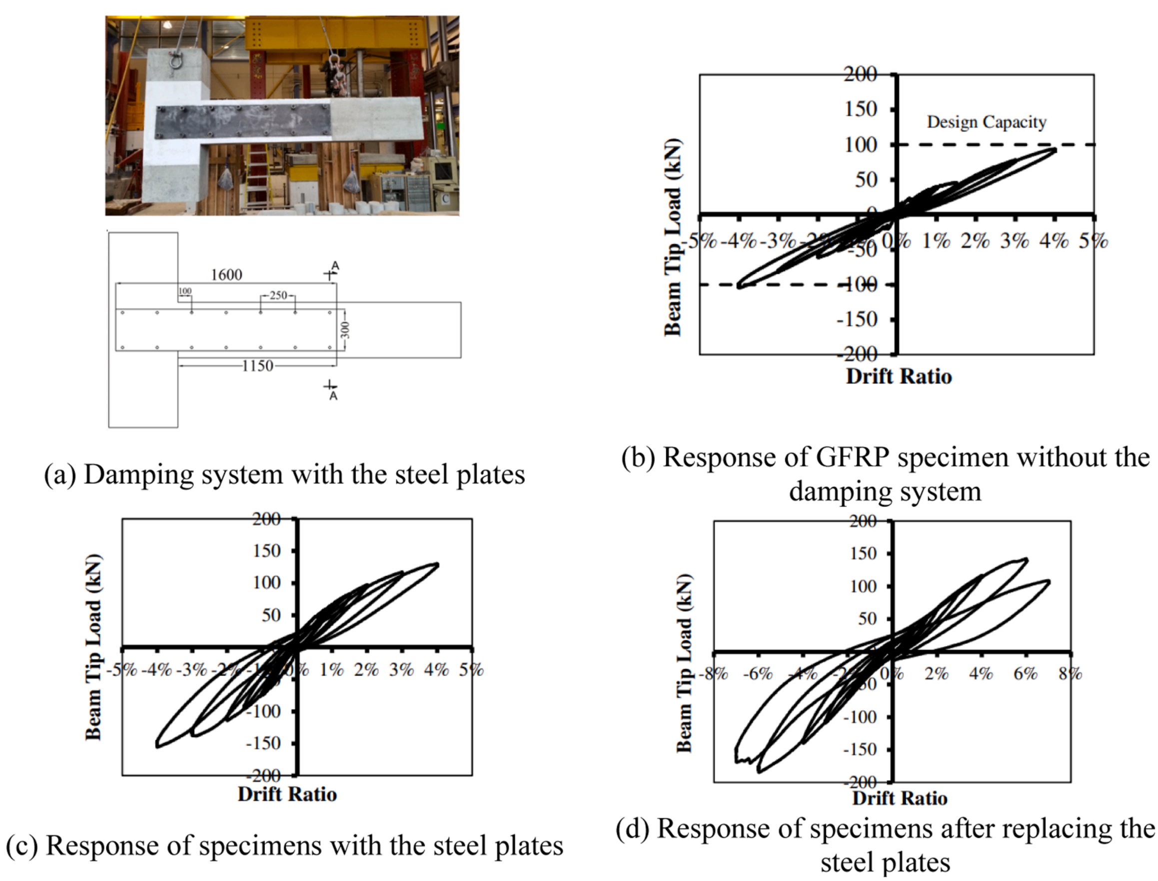

Fig. 20. Effect of damping system on the response of GFRP-RC MRF [107].

weight-to-strength ratio, they can be more attractive to the precast concrete industry, maximizing benefits in terms of accelerated construction under high-quality control with this durable solution. The comparison between cast-in-place and precast connection with GFRP demonstrated that precast beam-column sub-assemblages can perform in a way comparable to cast-in-place one [108]. Particularly in harsh environments where the possibility of steel corrosion is high, such as in jetties where casting concrete in situ can be challenging, GFRP-reinforced precast structures can find good applications. Tests on beam-column subassemblies in MRFs of jetties subjected to cyclic loads have recently been initiated, revealing the same drawbacks identified in cast-in-place structures [109,110]. The guidelines for designing connections of precast structures with conventional steel were found to be unsuitable for extension to GFRP-RC structures [111]. The global response of precast GFRP-RC MRF of jetties in terms of capacity, stiffness, and energy dissipation capacity depended on the connection details [112,113]. Recently, there has been a marked increase in demand for advanced and efficient connection details in precast construction [109,114]. This demand arises from the need to meet accelerated construction requirements while incorporating external damper systems seamlessly for enhanced seismic performance [115,116]. Since research on the connection of precast GFRP-RC MRFs is at an early stage, defined drawbacks in cast-in-place MRFs, mainly due to low stiffness, ductility, and poor energy dissipation of GFRP-RC structures, should be considered when developing connection systems. This can achieve optimum structures in terms of durability, accelerated construction, and satisfactory cyclic performance.

8. Conclusions

The study conducted a comprehensive review of the seismic performance of GFRP-RC MRF. A thorough comparison was made between the seismic performance of GFRP-RC and steel-RC beam-column sub-assemblages, considering various aspects such as strength, ductility, stiffness, energy dissipation, and residual damage. The analysis also delved into the impact of critical parameters on the beam-column sub-assemblages' response. The use of GFRP as both longitudinal and transverse reinforcement in MRF was revealed. In summary, the key conclusions drawn from this investigation are:

1. The hysteresis response of GFRP-RC beam-column sub-assemblages showed narrow hysteresis loops with the ability to reach higher drifts without degradation. The concentrated plastic hinge due to local yielding of steel was replaced with cracks spread along a larger portion in GFRP-RC MRFs with the advantage to achieve its design capacity after repeated earthquakes load while revealing its functionality after earthquakes with minimal damage.
2. With achieving the strong column weak beam concept and well confine the joint region, the GFRP-RC beam-column sub-assemblages are able to reach the design capacity and withstand minimum drift ratios of 4 %. This confirms that GFRP-RC MRFs can be designed to satisfy both strength and deformation capacity with ensuring gradual failure with some level of ductility. A value of 75 % of the design capacity should be considered at the design drift ratio of 2.5 % that usually adopted for RC structures.
3. Although GFRP-RC MRFs can be designed to achieve the target capacity with minimal damage, it comes with a cost on its stiffness and energy dissipation capacity. However, brittle failure of GFRP bars can be avoided and changed to gradual failure when implemented in MRFs if an upper limit of reinforcement stress is considered instead of the full capacity of the bars. This can be achieved by providing a larger reinforcement amount.
4. While GFRP bars are elastic, GFRP-RC beam-column subassemblies showed inelastic behaviour with some energy dissipation. However, this dissipated energy is significantly less than those in steel-RC. On the other hand, at the structural level, the overall energy dissipation of GFRP-RC MRFs is not significantly lower than that of steel-RC MRFs and is sometimes comparable. Also, by improving the concrete material and design, the level of energy dissipation can be further improved.
5. Presence of slab floor and lateral beams have a significant impact on improving the connection performances in terms of capacity, stiffness, and energy dissipation. Although the presence of lateral beams enhanced the contribution of the slab by increasing the effective slab width, the effective slab width in GFRP-RC was less than that of with steel reinforcement.
6. While lateral beams and floor slabs enhance the connection performance, higher axial loads and increased joint aspect ratio can have a negative impact. However, among the factors influencing the connection performance, concrete strength, the provision of joint shear reinforcement, and adequate anchorage of the beam bars are considered the most critical in determining joint shear strength.
7. Joint shear strength can be enhanced by the provision of joint shear reinforcement in the form of horizontal stirrups, spirals, or x-shape reinforcement. Exterior connections with confining stirrups were able to resist shear stress of $0.85\sqrt{f_c'}$ and $1.3\sqrt{f_c'}$ without and with lateral beams, respectively. While interior connection with lateral beams was able to resist shear stress of $1.8\sqrt{f_c'}$. However, the evaluation of the minimum required amount of reinforcement to achieve that value is yet to be investigated.
8. For proper design of the joint region in GFRP-RC MRFs, the following design criteria can be considered:
   - Strong column weak beam should be achieved by ensuring column's flexural capacity 20% greater than the beam's flexural capacity.
   - As long as joint shear failure is avoided and a strong column-week beam concept is adopted, a higher beam reinforcement ratio is recommended to enhance the stiffness and energy dissipation of GFRP-RC connections.
   - Minimum straight anchorage length of 24d should be provided to prevent slippage of beam bars. Otherwise, the 90-degree standard hooked or headed anchorage can be effectively used.
   - Joint shear stress should be limited to the maximum joint shear capacity reported in this study. However, 75 % of the design capacity should be considered at the design drift ratio of 2.5 % which is usually adopted for RC structures.
   - Sufficient joint shear reinforcement should be provided in the joint region to ensure the development of the joint shear capacity.

Future research

To further improve the seismic performance of GFRP-RC MRFs, studies are encouraged to investigate the effect of better concrete confinement and the use of fibre-reinforced concrete or ductile concrete to improve the compression-controlled mechanism and accordingly partially mitigate the reduced ductility and energy dissipation of GFRP-RC members. Furthermore, the incorporation of external damping systems is encouraged to address the low energy dissipation capacity. Further research is also encouraged to investigate the effect of joint aspect ratio, a wide range of column axial loads, and different arrangements and amounts of joint reinforcement to refine the required amount of joint reinforcement for achieving the connection capacity. Accurate analytical models can then be developed to predict joint shear strength and establish minimum detailing provisions for connections to achieve that capacity. Addressing these aspects holds the potential to aid in establishing seismic provisions within international standards, ensuring the proper performance of MRFs.

CRediT authorship contribution statement

Mohamed H. El-Naqeeb: Writing – original draft, Formal analysis, Conceptualization, Methodology, Investigation, Visualization. **Reza Hassanli**: Writing – review & editing, Supervision, Project administration, Methodology, Conceptualization. **Yan Zhuge**: Writing – review & editing, Supervision. **Xing Ma**: Writing – review & editing, Supervision. **Milad Bazli**: Writing – review & editing, Supervision. **Allan Manalo**: Writing – review & editing, Supervision.

Declaration of Competing Interest

The authors declare that they have no known competing financial interests or personal relationships that could have appeared to influence the work reported in this paper.

References

[1] Paulay T. Joints in Reinforced Concrete Frames Designed Earthquake Resistance. U SN Z-Japan Seminar Report1984.
[2] El-Metwally S, Chen W-F. Structural concrete: strut-and-tie models for unified design. CRC Press; 2017.
[3] Saatcioglu M, Mitchell D, Tinawi R, Gardner NJ, Gillies AG, Ghobarah A, et al. The August 17, 1999, Kocaeli (Turkey) earthquake damage to structures. Can J Civ Eng 2001;28:715–37.
[4] Hassan WM. Analytical and experimental assessment of seismic vulnerability of beam-column joints without transverse reinforcement in concrete buildings. Berkeley: University of California; 2011.
[5] ACI-ASCE Committee 352R. Recommendations for design of beam-column connections in monolithic reinforced concrete. Farmington Hills, Michigan: American Concrete Institute; 2002.
[6] EN 1998-1. Eurocode 8: Design of structures for earthquake resistance Part 1: General rules, seismic actions and rules for buildings. The European Union Per Regulation 305/2011, Directive 98/34/EC, Directive 2004/18/EC, Brussels; 2004.
[7] Committee A. Building code requirements for structural concrete (ACI 318-19) and commentary. American Concrete Institute; 2019.
[8] Park R. Ductile design approach for reinforced concrete frames. Earthq Spectra 1986;2:565–619.
[9] Huang L, Ye H, Jin X, Jin N, Xu Z. Corrosion-induced shear performance degradation of reinforced concrete beams. Constr Build Mater 2020;248:118668.
[10] Alaskar A, Alqarni AS, Alfalah G, El-Sayed AK, Mohammadhosseini H, Alyousef R. Performance evaluation of reinforced concrete beams with corroded web reinforcement: experimental and theoretical study. J Build Eng 2021;35:102038.
[11] Manalo A, Mendis P, Bai Y, Jachmann B, Sorbello C. Fiber-reinforced polymer bars for concrete structures: state-of-the-practice in Australia. J Compos Constr 2021;25:05020007.
[12] Wasim M, Ngo TD, Abid M. Investigation of long-term corrosion resistance of reinforced concrete structures constructed with various types of concretes in marine and various climate environments. Constr Build Mater 2020;237:117701.
[13] Dagdag O, Hsissou R, El Harfi A, Berisha A, Safi Z, Verma C, et al. Fabrication of polymer based epoxy resin as effective anti-corrosive coating for steel: computational modeling reinforced experimental studies. Surf Interfaces 2020; 18:100454.
[14] Sari MG, Ramezanzadeh B. Epoxy composite coating corrosion protection properties reinforcement through the addition of hydroxyl-terminated hyperbranched polyamide non-covalently assembled graphene oxide platforms. Constr Build Mater 2020;234:117421.
[15] Cao H, Lyu Z, Dong W, Zhao Z, Gan W, Wang Y. Corrosion experimental research on local damage of epoxy-coated steel bars in concrete under marine environment. Front Mater 2022;8:821716.
[16] Gudonis E, Timinskas E, Gribniak V, Kaklauskas G, Arnautov AK, Tamulėnas V. FRP reinforcement for concrete structures: state-of-the-art review of application and design. Eng Struct Technol 2013;5:147–58.
[17] Muda MF, Hashim MHM, Kamarudin MK, Mohd MH, Tafsirojjaman T, Rahman MA, et al. Burst pressure strength of corroded subsea pipelines repaired with composite fiber-reinforced polymer patches. Eng Fail Anal 2022;136: 106204.
[18] Duo Y, Liu X, Liu Y, Tafsirojjaman T, Sabbrojjaman M. Environmental impact on the durability of FRP reinforcing bars. J Build Eng 2021;43:102909.
[19] Rajak DK, Pagar DD, Menezes PL, Linul E. Fiber-reinforced polymer composites: manufacturing, properties, and applications. Polymers 2019;11:1667.
[20] Yu P, Silva P, Nanni A. Flexural strengthening of RC beams using GFRP grid bonded with sprayed polyurea. Eng Struct 2023;292:116516.
[21] Qian K, Li B. Strengthening and retrofitting precast concrete buildings to mitigate progressive collapse using externally bonded GFRP strips. J Compos Constr 2019; 23:04019018.
[22] Ayash NM, Abd-Elrahman AM, Soliman A-E. Repairing and strengthening of reinforced concrete cantilever slabs using Glass Fiber–Reinforced Polymer (GFRP) wraps. Struct: Elsevier 2020:2488–506.
[23] Zhou A, Chow CL, Lau D. Structural behavior of GFRP reinforced concrete columns under the influence of chloride at casting and service stages. Compos Part B: Eng 2018;136:1–9.
[24] Zakkaria MFM, Shanmugam P. Flexural behavior of fiber-reinforced concrete beams with GFRP rebars under marine environmental conditions. Int J Adv Manuf Technol 2023:1–12.
[25] ACI 440.1R. Guide for the design and construction of structural concrete reinforced with fiber-reinforced polymer bars. American Concrete Institute; 2015.
[26] Khorasani AM, Esfahani MR, Sabzi J. The effect of transverse and flexural reinforcement on deflection and cracking of GFRP bar reinforced concrete beams. Compos Part B: Eng 2019;161:530–46.
[27] Al-Sunna R, Pilakoutas K, Hajirasouliha I, Guadagnini M. Deflection behaviour of FRP reinforced concrete beams and slabs: an experimental investigation. Compos Part B: Eng 2012;43:2125–34.
[28] Gouda O, Asadian A, Galal K. Flexural and serviceability behavior of concrete beams reinforced with ribbed GFRP bars. J Compos Constr 2022;26:04022064.
[29] Mirmiran A, Yuan W, Chen X. Design for slenderness in concrete columns internally reinforced with fiber-reinforced polymer bars. Struct J 2001;98: 116–25.
[30] Yan F, Lin Z, Yang M. Bond mechanism and bond strength of GFRP bars to concrete: a review. Compos Part B: Eng 2016;98:56–69.
[31] Henin E, Morcous G. Bond behavior of helically wrapped sand coated deformed Glass Fiber-Reinforced Polymer (GFRP) bars in concrete. Constr Build Mater 2021;288:123120.
[32] Lu J, Afefy HM, Azimi H, Sennah K, Sayed-Ahmed M. Bond performance of sand-coated and ribbed-surface glass fiber reinforced polymer bars in high-performance concrete. Struct: Elsevier 2021:10–9.
[33] Solyom S, Balázs GL. Bond of FRP bars with different surface characteristics. Constr Build Mater 2020;264:119839.
[34] ACI CODE 440.11-22: building code requirements for structural concrete reinforced with glass fiber-reinforced polymer (GFRP) bars-code and commentary. 1st printing. Farmington Hills, MI: American Concrete Institute (ACI); 2022.
[35] El-Nemr A, Ahmed EA, El-Safty A, Benmokrane B. Evaluation of the flexural strength and serviceability of concrete beams reinforced with different types of GFRP bars. Eng Struct 2018;173:606–19.
[36] Aghdasi P, Heid AE, Chao S-H. Developing ultra-high-performance fiber-reinforced concrete for large-scale structural applications. Acids Mater J 2016; 113.
[37] Elshamandy MG, Farghaly AS, Benmokrane B. Experimental behavior of glass fiber-reinforced polymer-reinforced concrete columns under lateral cyclic load. Acids Struct J 2018;115:337–49.
[38] Mohamed N, Farghaly AS, Benmokrane B, Neale KW. Drift capacity design of shear walls reinforced with glass fiber-reinforced polymer bars. Acids Struct J 2014;111:1397.
[39] Eladawy M, Hassan M, Benmokrane B, Ferrier E. Lateral cyclic behavior of interior two-way concrete slab–column connections reinforced with GFRP bars. Eng Struct 2020;209:109978.
[40] Qian K, Xue T-Q, Deng X-F, Ma J. Experimental investigation on seismic behavior of Ultra-high performance concrete columns reinforced with GFRP bars. Struct: Elsevier 2023:568–80.
[41] Mady M, El-Ragaby A, El-Salakawy E. Experimental investigation on the seismic performance of beam-column joints reinforced with GFRP bars. J Earthq Eng 2011;15:77–98.
[42] Said A, Nehdi M. Use of FRP for RC frames in seismic zones: Part I. Evaluation of FRP beam-column joint rehabilitation techniques. Appl Compos Mater 2004;11: 205–26.
[43] Guo R, Yang D, Jia B, Tang D. Seismic response of GFRP-RC interior beam-to-column joints under cyclic static loads. Buildings 2022;12:1987.
[44] Ghomi SK, El-Salakawy E. Effect of joint shear stress on seismic behaviour of interior GFRP-RC beam-column joints. Eng Struct 2019;191:583–97.
[45] Sonobe Y, Fukuyama H, Okamoto T, Tanigaki M. Structural performances of concrete frame reinforced with FRP reinforcement. Concr Res Technol 1994;5: 103–13.
[46] Sharbatdar M., Saatcioglu M., Benmokrane B., El-Salakawy E. Behaviour of FRP reinforced concrete beam-column joints under cyclic loading. 3rd International Conference on Durability & Field Applications of Fibre Rein-forced Polymer (FRP) Composites for Construction,(CDCC-07), Quebec City, Quebec, Canada2007. p. 541-548.
[47] Said A, Nehdi M. Use of FRP for RC frames in seismic zones: Part II. Performance of steel-free GFRP-reinforced beam-column joints. Appl Compos Mater 2004;11: 227–45.
[48] S806:12C. Design and construction of building structures with fibre-reinforced polymers. Ontario, Canada: Canadian Standards Association; 2012.
[49] Code U.B.. Uniform building code. International Conference of Building Officials, Whittier, CA1997.
[50] ASoC Engineers. Minimum design loads and associated criteria for buildings and other structures. American Society of Civil Engineers; 2017.
[51] Ghomia SK, El-Salakawy E. Effect of geometrical configuration on seismic behavior of GFRP-RC beam-column joints. Adv Concr Constr 2020;9:313–26.
[52] Mady M, El-Ragaby A, El-Salakawy E. Seismic behavior of beam-column joints reinforced with GFRP bars and stirrups. J Compos Constr 2011;15:875–86.
[53] Yang K-H, Mun J-H. Cyclic flexural and shear performances of beam elements with longitudinal glass fiber reinforced polymer (GFRP) bars in exterior beam-column connections. Appl Sci 2018;8:2353.

[54] Ghomi SK, El-Salakawy E. Seismic performance of GFRP-RC exterior beam–column joints with lateral beams. J Compos Constr 2016;20:04015019.
[55] Ghomi SK, El-Salakawy EF. Cyclic behavior of glass fiber-reinforced polymer-reinforced concrete exterior beam-column-slab connections. Acids Struct J 2020; 117.
[56] Hopartean G, Donchev T, Petkova D, Georgopoulos C, Limbachiya M. Experimental investigation of concrete frames reinforced with GFRP bars under reversed cyclic loading. Eng Struct 2024;302:117377.
[57] Aliasghar-Mamaghani M, Khaloo A. Seismic behavior of concrete moment frame reinforced with GFRP bars. Compos Part B: Eng 2019;163:324–38.
[58] Hasaballa MH, El-Ragaby A, El-Salakawy EF. Seismic performance of exterior beam–column joints reinforced with glass fibre reinforced polymer bars and stirrups. Can J Civ Eng 2011;38:1092–102.
[59] Zhao Y, Zhang Y, Xu J, Yu P, Yu Q, Yin S. Seismic behavior and restoring force model of GFRP-RC beam-column interior joints. Struct: Elsevier 2022:955–68.
[60] Li VC, Wang S. Flexural behaviors of glass fiber-reinforced polymer (GFRP) reinforced engineered cementitious composite beams. Mater J 2002;99:11–21.
[61] Park R. Evaluation of ductility of structures and structural assemblages from laboratory testing. Bull NZ Soc Earthq Eng 1989;22:155–66.
[62] Pantelides CP, Clyde C, Reaveley LD. Performance-based evaluation of reinforced concrete building exterior joints for seismic excitation. Earthq Spectra 2002;18: 449–80.
[63] Nader Tehrani B, Narayan Prajapati G, Farghaly AS, Benmokrane B. Effect of confinement level and staggering on seismic performance of lap-spliced GFRP-reinforced concrete columns. J Compos Constr 2024;28:04024002.
[64] Safdar M, Sheikh MN, Hadi MN. Glass fiber-reinforced polymer-reinforced beam-column connections with novel connection details. Acids Struct J 2022;119: 271–86.
[65] Sonobe Y, Fukuyama H, Okamoto T, Kani N, Kimura K, Kobayashi K, et al. Design guidelines of FRP reinforced concrete building structures. J Compos Constr 1997; 1:90–115.
[66] Nanni A. Flexural behavior and design of RC members using FRP reinforcement. J Struct Eng 1993;119:3344–59.
[67] Jaeger L., Mufti A., Tadros G. The concept of the overall performance factor in rectangular-section reinforced concrete members. Proceedings of the 3rd International Symposium on Non-Metallic (FRP) Reinforcement for Concrete Structures, Sapporo, Japan1997. p. 551-559.
[68] Naaman A, Jeong M. 45 Structural ductility of concrete beams prestressed with FRP tendons. Non-Metallic (FRP) Reinforcement for concrete structures: proceedings of the second international RILEM symposium. Boca Raton, FL, USA: CRC Press; 1995. p. 379.
[69] Kharal Z. Towards understanding the seismic behaviour of GFRP confined concrete columns. Canada: University of Toronto; 2019.
[70] Sleiman N, Polak MA. Experimental study on GFRP-reinforced concrete closing knee joints. J Compos Constr 2020;24:04020022.
[71] Saravanan J, Kumaran G. Joint shear strength of FRP reinforced concrete beam-column joints. Open Eng 2011;1:89–102.
[72] Hasaballa M, El-Salakawy E. Shear capacity of exterior beam-column joints reinforced with GFRP bars and stirrups. J Compos Constr 2016;20:04015047.
[73] El-Mandouh MA, Omar MS, Elnaggar MA, Abd El-Maula AS. Cyclic behavior of high-strength lightweight concrete exterior beam-column connections reinforced with GFRP. Buildings 2022;12:179.
[74] Chen G, Hadi MN, Gao D, Zhao L. Experimental study on the properties of corroded steel fibres. Constr Build Mater 2015;79:165–72.
[75] Granju J-L, Balouch SU. Corrosion of steel fibre reinforced concrete from the cracks. Cem Concr Res 2005;35:572–7.
[76] Rezaee Azariani H, Shariatmadar H, Esfahanir MR. Exterior concrete beam-column connection reinforced with glass fiber reinforced polymers (GFRP) bars under cyclic loading. AUT J Civ Eng 2018;2:161–76.
[77] Lin G, Zeng J-J, Liang S-D, Liao J, Zhuge Y. Seismic behavior of novel GFRP bar reinforced concrete beam-column joints internally reinforced with an FRP tube. Eng Struct 2022;273:115100.
[78] Safdar M, Sheikh MN, Hadi MN. Effect of connection transverse reinforcement on the behavior of GFRP-RC T-connections: numerical investigation. Constr Build Mater 2023;363:129827.
[79] Hwang S-J, Hung-Jen L, Liao T-F, Kuo-Chou W, Tsai H-H. Role of hoops on shear strength of reinforced concrete beam-column joints. Acids Struct J 2005;102:445.
[80] Hegger J, Sherif A, Roeser W. Nonseismic design of beam-column joints. Struct J 2003;100:654–64.
[81] Bakir P, Boduroğlu H. A new design equation for predicting the joint shear strength of monotonically loaded exterior beam-column joints. Eng Struct 2002; 24:1105–17.
[82] El-Naqeeb MH, Abdelwahed BS, El-Metwally SE. Numerical investigation of RC exterior beam-column connection with different joint reinforcement detailing. Struct: Elsevier 2022:1570–81.
[83] Safdar M, Sheikh MN, Hadi MN. Cyclic performance of GFRP-RC T-connections with different anchorage and connection details. J Compos Constr 2022;26: 04022022.
[84] Cosgun C, Turk AM, Mangir A, Cosgun T, Kiymaz G. Experimental behaviour and failure of beam-column joints with plain bars, low-strength concrete and different anchorage details. Eng Fail Anal 2020;109:104247.
[85] Jeremic N, Sheikh SA. Performance of glass fiber-reinforced polymer bent bars. Acids Struct J 2021.
[86] Mady M., Hasaballa M., El-Ragaby A., El-Salakawy E. Effect of reinforcement detailing on the behavior of GFRP-RC beam-column joints. Advances in FRP Composites in Civil Engineering: Proceedings of the 5th International Conference on FRP Composites in Civil Engineering (CICE 2010), Sep 27–29, 2010, Beijing, China: Springer; 2011. p. 330-333.
[87] Balamuralikrishnan R, Saravanan J. Finite element analysis of beam-column joints reinforced with GFRP reinforcements. Civ Eng J 2019;5:2708–26.
[88] Hasaballa M, El-Salakawy E. Anchorage performance of GFRP headed and bent bars in beam-column joints subjected to seismic loading. J Compos Constr 2018; 22:04018060.
[89] El-Naqeeb MH, El-Metwally SE, Abdelwahed BS. Performance of exterior beam-column connections with innovative bar anchorage schemes: numerical investigation. Structures 2022;44:534–47.
[90] Hamil SJ. Reinforced concrete beam-column connection behaviour. Durham University; 2000.
[91] Scott RH. Intrinsic mechanisms in reinforced concrete beam-column connection behavior. Struct J 1996;93:336–46.
[92] Ghomi SK, El-Salakawy E. Seismic behavior of exterior GFRP-RC beam–column connections: analytical study. J Compos Constr 2018;22:04018022.
[93] Safdar M, Sheikh MN, Hadi MN. Numerical study on shear strength of GFRP-RC T-Joints. Struct: Elsevier 2022:926. 43.
[94] Safdar M, Sheikh MN, Hadi MN. Finite element analysis to predict the cyclic performance of GFRP-RC exterior joints with diagonal bars. J Build Eng 2023;65: 105774.
[95] El-Naqeeb M, El-Metwally S, Abdelwahed B. Strength of exterior beam-column connections considering column axial stress: numerical investigation. Jordan J Civ Eng 2022;16.
[96] Ghomi SK, El-Salakawy E. Seismic behavior of GFRP-reinforced concrete interior beam–column–slab subassemblies. J Compos Constr 2019;23:04019047.
[97] Hassanli R, Manalo A, Vafaei D, Yekrangnia M, Elchalakani M, Noël M. Cyclic behavior of GFRP-reinforced concrete one-way slabs with synthetic fibers. J Build Eng 2023;65:105741.
[98] Standard C. Design and construction of building components with fibre-reinforced polymers. S806-02, Canadial Standards Association. 2002.
[99] Canadian Standards Association (CSA) (2017), Design and Construction of Building Structures with Fibre Reinforced Polymers. CAN/CSA-S806-12, Canadian Standards Association, Ontario, Canada; 2017.
[100] AASHTO. AASHTO LRFD bridge design guide specifications for GFRP–reinforced concrete. American Association of State Highway and Transportation Officials; 2018.
[101] 203/2006C-D. Guide for the design and construction of concrete structure reinforced with fiberreinforced polymer bars. Rome: National Research Council; 2007.
[102] JSCE. Recommendation for design and construction of concrete structures using continuous fiber reinforcing materials: Japan Soc. of Civil Engineers Tokyo, Japan; 1997.
[103] Sadeghi M, Jandaghi Alaee F, Akbarzadeh Bengar H, Jafari A. Evaluating the efficiency of supplementary rebar system in improving hysteretic damping of self-centering rocking walls. Bull Earthq Eng 2022;20:6075–107.
[104] Naserpour A, Fathi M, Dhakal RP. Numerical analysis of inclined demountable precast concrete walls with rocking-based composite columns for seismic protection of building structures. J Build Eng 2023;75:107009.
[105] Lu Y-T, Guo Z-X, Liu Y, Basha SH. Performance of prefabricated RC column with replaceable column-base connection under cyclic lateral loads. Eng Struct 2021; 240:112343.
[106] Javan D, Kheyroddin A, Dabiri H, Esfahani MR. Performance of RC beam-column joints with hybrid GFRP-steel reinforcement under cyclic and axial loads. Struct: Elsevier 2023:1408–15.
[107] Ghomi SK, El-Salakawy E. Seismic performance improvement of GFRP-RC moment frames. Can J Civ Eng 2020;47:704–17.
[108] Ngo TT, Pham TM, Hao H, Chen W, San Ha N. Proposed new dry and hybrid concrete joints with GFRP bolts and GFRP reinforcement under cyclic loading: Testing and analysis. J Build Eng 2022;49:104033.
[109] El-Naqeeb MH, Ghanbari-Ghazijahani T, Gholampour A, Hassanli R, Zhuge Y, Ma X, et al. Cyclic behaviour of an innovative cap beam to column pocketless connection in GFRP-RC precast structures. Structures 2024;61:106003.
[110] Ghanbari-Ghazijahani T, Hassanli R, Manalo A, Smith ST, Vincent T, Gravina R, et al. Cyclic behavior of beam–column pocket connections in GFRP-reinforced precast concrete assemblages. J Compos Constr 2023;27:04022107.
[111] El-Naqeeb MH, Hassanli R, Zhuge Y, Ma X, Manalo A. Numerical investigation on the behaviour of socket connections in GFRP-reinforced precast concrete. Eng Struct 2024;303:117489.
[112] Hassanli R, Vincent T, Manalo A, Smith ST, Gholampour A, Gravina R, et al. Connections in GFRP reinforced precast concrete frames. Compos Struct 2021; 276:114540.
[113] Hassanli R, Vincent T, Manalo A, Smith ST, Gholampour A, Gravina R. Large-scale experimental study on pocket connections in GFRP-reinforced precast concrete frames. Struct: Elsevier 2021:523–41.
[114] El-Naqeeb MH, Hassanli R, Zhuge Y, Ma X, Bazli M, Manalo A. Performance of GFRP-RC precast cap beam to column connections with epoxy-anchored reinforcement: a numerical study. Arch Civ Mech Eng 2024;24:131.
[115] Kenarkoohi M, Hassan M. Review of accelerated construction of bridge piers-methods and performance. Adv Bridge Eng 2024;5:3.
[116] Bi K, Li C, Hao H. State-of-the-art review of the seismic performance of precast segmental columns. Adv Bridge Eng 2022;3:7.